Materials Today Communications 32 (2022) 104036

Contents lists available at ScienceDirect

Materials Today Communications

journal homepage: www.elsevier.com/locate/mtcomm

Consolidation of continuous-carbon-fiber-reinforced PAEK composites: a review

R. Arquier, I. Iliopoulos, G. Régnier, G. Miquelard-Garnier *

Laboratoire PIMM, Arts et Métiers Institute of Technology, CNRS, CNAM, HESAM Universite, 151 Boulevard de l'Hôpital, 75013 Paris, France

ARTICLE INFO

Keywords:
PAEK
Carbon fibers
High-performance thermoplastic composites
Consolidation
Tape lay-up
Out-of-autoclave process
"in-situ" consolidation
Squeeze flow

ABSTRACT

Continuous-Carbon-Fiber (CF)/polyaryletherketone (PAEK) composites have recently attracted interest especially in the aerospace industry due to short-time processes and possible weldability and recyclability. However, their manufacturing remains challenging as it involves several steps such as tape fabrication, tape lay-up and consolidation. This last step mainly aims at achieving a sufficiently low void content composite to obtain the desired mechanical properties. To become an economically viable alternative over classical thermoset-based composites, "in-situ" or out-of-autoclave (OOA) consolidation processes have to become part of the manufacturing process of CF/PAEK. These techniques have, for now, some limitations which lead to difficulties in producing parts of the same quality as autoclave consolidated ones. Understanding the multi-scale rheological phenomena involved during consolidation is therefore critical, which constitutes the main goal of this review. Reflecting on the literature, guides for improving the OOA and "in-situ" consolidation, both in terms of process and materials, are finally suggested.

1. Introduction

For many decades, thermoset based composites such as carbon fiber (CF)/polyimide, CF/phtanolonitrile or CF/bismaleimide were used in the aerospace sector due to their ease of processing (e.g. low viscosities and long pot-life [1,2]), high service temperatures [3–5] and excellent mechanical properties [2]. However, the sometimes-consequent curation times under energy-intensive process devices and limited shelf life [6] coupled with an increase in industrial demands are gradually making thermoset-based composites less competitive than high-performance thermoplastic ones. These new materials respond to the economic challenges as well as having potential recyclability and weldability [7,8].

The PAEK family is a common example of such high-performance thermoplastics, with high service temperature, high chemical and oxidation resistance, good impact properties, non-flammable behavior and weldability [9–11]. For PAEK matrix-based composites, the filler is generally carbon fiber in order to maximize stiffness, thermal and electrical conductivity of the final component [12] while reducing its total weight. In the aerospace industry, continuous fiber reinforcement is often used to increase the specific strength of the whole material.

The manufacturing process of these composites includes a phase of prepreg (PREimPREGnated) or tape fabrication, i.e. the fabrication of a composite film with typical thickness on the order of a few hundred microns. Then a phase of tape placement aims at stacking tapes with the desired fiber orientation. Finally, a consolidation step aims at welding the tapes together and lowering the void content by applying pressure at high temperature, both within the tapes (intra-laminar voids) and in-between them (inter-laminar voids). This is necessary since, for example in the aerospace industry, the final composite piece must have a porosity level lower than 1% [13,14]. All these steps involve similar and coupled physicochemical mechanisms such as melting/crystallization of the matrix, rearrangement of the fibers depending on rheological properties and local flows, polymeric chains interdiffusion and crystallization at the interfaces, voids formation or disappearance …, which in turn all lead to complex structure/properties relationships in the composite parts.

The different PAEK and CF have been reviewed by Veazey et al. [12] while the state-of-the-art of thermoplastic composites manufacturing processes has been the subject of many reviews, such as the one by Vaidya et al. [8] or more recently by Boon et al. [15]. Khaled et al. [16], Pérez-Martín et al. [17] and Martin et al. [18], which focused on the physical phenomena (crystallinity, adhesion, degradation) occurring during processing for such composites. However, according to the authors' knowledge, while consolidation is now relatively well-understood

* Corresponding author.
E-mail address: guillaume.miquelardgarnier@lecnam.net (G. Miquelard-Garnier).

https://doi.org/10.1016/j.mtcomm.2022.104036
Received 11 April 2022; Received in revised form 22 June 2022; Accepted 14 July 2022
Available online 16 July 2022

Nomenclature

AFP	Automatic Fiber Placement.
ATL	Automatic Tape Laying.
ATP	Automated Tape Placement.
b and e	Width and Thickness of the sample (m).
CF	Carbon Fibers.
CFRTP	Carbon-Fiber-Reinforced Thermoplastic.
CY	Cytec.
D_{IC}	Degree of Intimate Contact.
E	Young's modulus (MPa).
F	Force applied (N).
G_{IC}	Mode I Interlaminar fracture toughness (J/m^2).
G'_L and G''_L	Storage and Loss Moduli along the fibers respectively (Pa).
G'_T and G''_T	Storage and Loss Moduli in the transverse direction of the fibers respectively (Pa).
GF/PP	Glass Fiber/Polypropylene.
h, h_0	Half distance and half initial distance between plates respectively (m).
$\dot{h}$	Squeeze rate (m/s).
HGT	Hot gas torch.
l_0	Initial half-length of the specimen (m).
I_L and I_T	Longitudinal and Transverse second moment of area respectively (m^4).
ILSS	InterLaminar Shear Strength (MPa).
L_0 and L	Initial length and length of the specimen respectively (m).
LSS	Lap Shear Strength (MPa).
m and n	Coefficients of the power-law viscosity model (m in Pa.s^n and n without unit).
M and M_0	Torque and amplitude of the torque respectively.
OOA	Out-Of-Autoclave.
PAEK	Polyaryletherketone.
PEEK	Polyetheretherketone.
PEI	Polyetherimide.
PEKK	Polyetherketoneketone.
PPS	PolyPhenylene Sulfide.
R	Radius of the plates (m).
t	Time (s).
T_g	Glass transition Temperature (°C or K).
T_m	Melting Temperature (°C or K).
TC	TenCate.
T/I	Terephtaloyle and Isophtaloyle ratio.
UD	UniDirectional.
US	Ultrasonic.
USSW	UltraSonic Spot Welding.
VBO	Vacuum Bagging Only.
W_0	Initial half width of the specimen (m).
W	Width of the specimen (m).
γ_L	Shear along the fibers.
γ_T	Shear transverse to the fibers.
$\dot{\gamma}$	Shear rate (s^{-1}).
δ	Phase angle.
Δ	Correction factor (m).
η	Viscosity (Pa.s).
η_T and η_{T0}	Transverse and Apparent transverse viscosity (Pa.s).
Θ	Amplitude of the twist angle.
λ	Relaxation time (s).
σ_y	Yield stress (MPa).
ω	Angular frequency (rad/s).

for thermosets-based composites [19], it is not the case for Carbon-Fiber-Reinforced Thermoplastics (CFRTP), typically CF/PAEK, because of a more complex rheological behavior [20].

The objective of this review is then to get a better insight on the consolidation step of CF/PAEK composites, crucial for the obtention of high-quality parts. After a brief section recalling the main features of the materials and the different steps of the composite manufacturing, the rheology of the material during consolidation will be presented and discussed in details. A last section will focus on possible ways, both in terms of materials and process, to improve the final consolidation quality.

2. Materials and composite manufacturing process

This part briefly recalls the main features of the materials used as well as the main steps in the manufacturing process of continuous CF/PAEK composites, i.e. prepreg manufacturing, lay-up and consolidation.

2.1. Polymer matrix

Amid the PAEK family, polyetheretherketone (PEEK), which has a glass transition temperature (T_g) and a melting temperature (T_m) of 143 °C and 340 °C respectively, has been vastly studied [21]. Over the last few decades, a significant amount of research has also been conducted on polyetherketoneketone (PEKK). PEEK and PEKK (see Fig. 1) have similar mechanical properties but commercially available PEKK

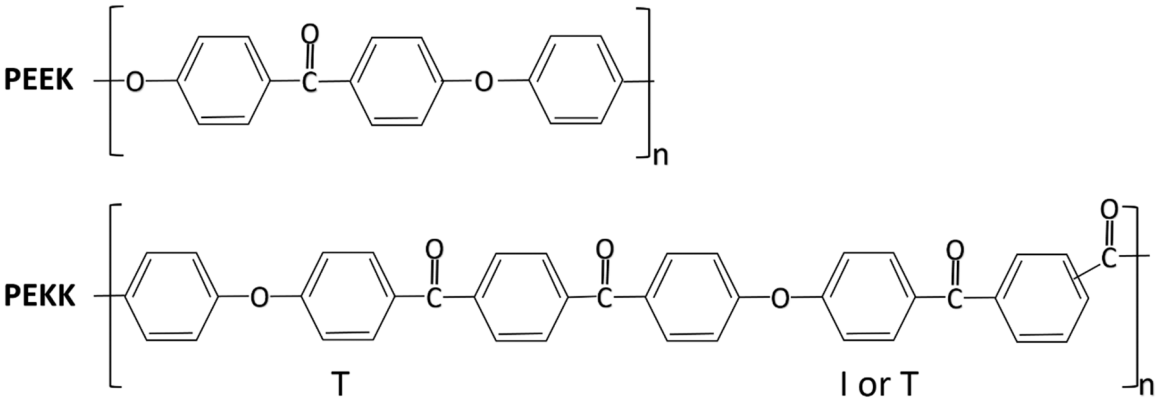

Fig. 1. Chemical structure of PEEK and PEKK.

processing temperature (i.e. its melting temperature T_m) can be reduced down to 300 °C while maintaining a high service temperature (i.e. its glass transition temperature T_g) by decreasing the ratio between terephtaloyl (para) and isophtaloyl (meta) isomers, known as the T/I ratio [12,22]. PEEK and PEKK T_g and T_m, for different T/I ratios, are given in Table 1.

Optimizing the copolymer composition is then needed to achieve a balance between ease of processing and mechanical properties for a given application, both in terms of temperatures and degree of crystallinity. Increasing the crystallinity (from 28% for PEKK 6000 and 7000–34% for PEKK 8000 [17,24], while it is close to 40% for PEEK [25] as shown in Table 1) results, as usual, in an increase in the Young's modulus E and yield stress σ_y but in a decrease in the strain at break. This effect of an increase in crystallinity on the mechanical properties has been confirmed for PEKK [22] and CF/PEEK [25].

Nowadays, most of the PAEK industrial production as well as academic research on CF reinforced high-performance thermoplastics focus on PEEK and PEKK, though other PAEK have been listed by Veazey et al. [12]. In consequence, the vast majority of results presented in the following will deal with either PEEK or PEKK, but should be generally applicable to other PAEK.

2.2. Fibers

Carbon fibers have a low density (about 1800 kg/m^3), high tensile strength (3–7 GPa) and modulus (200–500 GPa), with a diameter typically between 5 and 10 μm [26]. Fiber aspect ratio, orientation of fibers and fiber volume fraction play an important role on the composite mechanical properties [27–29]. Surface treatment of the carbon fibers is a classical way of modifying their inert surface and often used to improve matrix-fiber adhesion [30–32]. Veazey et al. [12] mention four possible treatments: sizing (i.e. coating with another polymer such as polyetherimide PEI), plasma treatment, electrochemical oxidation and grafting. Fig. 2 illustrates for example fiber-matrix debonding in an unsized CF/PEEK specimen.

Hsiao et al. [34] stated that the presence of carbon fibers has a weak influence on the crystallization kinetics of the PEKK matrix. More precisely, Pérez-Martín et al. [17] and Choupin et al. [35] concluded that for CF/PEKK (600X), the crystallization kinetics are similar than for the neat polymer at temperatures below 265 °C but faster above 265 °C, due to transcrystallinity at the fiber surface. Nonetheless, the degree of crystallinity of the composites remains close to the one of the matrix whether for PEKK [35] or PEEK [17,25].

2.3. Tape manufacturing

The impregnation step consists in infusing the matrix through the fibers and leads to the fabrication of a single {matrix + fibers} ply. The quality, structure and thermomechanical properties of the tape influence the next processing steps, so the impregnation step must be perfectly controlled [36].

The tape (or prepreg) manufacturing process is illustrated in Fig. 3:

The ply thickness, usually of the order of 200 μm, has been reduced to 20 μm in recent works [38–40]. Decreasing the ply thickness brings a more homogeneous and uniform prepreg, which can lead to better mechanical properties for the composite [41].

Table 1
Glass transition and melting temperatures, and degree of crystallinity of PEEK and of PEKK (600X, 700X and 800X are different grades produced by Arkema, related to the T/I ratio. For example, PEKK 700X stands for a proportion of 70% of T and 30% of I) [17,21,23–25].

	PEEK	*PEKK 600X*	*PEKK 700X*	*PEKK 800X*
T_g (°C)	*143*	*160*	*162*	*165*
T_m (°C)	*340*	*305*	*332*	*358*
χ (%)	*40*	*28*	*28*	*34*

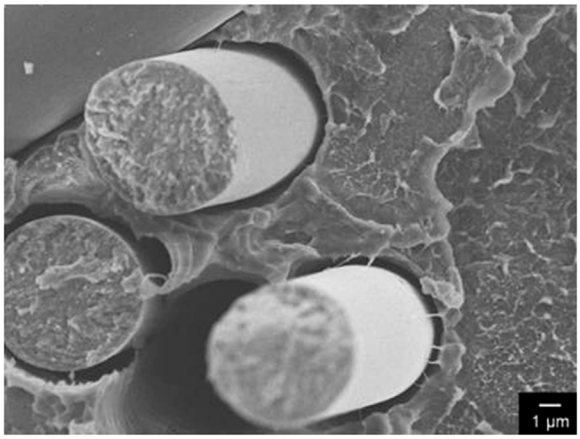

Fig. 2. Scanning electron microscopy image of a fiber-matrix debonding on an unsized CF/PEEK composite
Reprinted from Giraud et al. [33], ©2013 with permission from Elsevier.

2.4. Lay-up

A lay-up step, consisting in stacking a specific number of tapes with the desired fiber orientations, is necessary to obtain a composite part with the defined thickness. Unidirectional (UD) fiber composites exhibit outstanding mechanical properties in the fiber direction, sometimes better than metallic alloys, as reported in [12] concerning the ultimate tensile strength. However, Young's modulus or yield stress are only slightly higher than those of the matrix in the fiber transverse direction. Thus, to obtain a material with quasi-isotropic mechanical properties, each ply is usually stacked with fibers at 45° from the fibers of the previous ply.

To achieve the productivity required in the aerospace industry [13,42], new automated lay-up techniques have arisen, such as Automated Tape Placement (ATP). ATP process consists in placing tapes automatically on top of each other as shown in Fig. 4. For each tape deposited, the heat source (hot gas torch early on, and mainly laser and IR heating now [43]) melts the matrix near the nip point, i.e. where the incoming tape is in contact with the previous ply. At the same time, a silicone or metallic roller compresses the whole piece in order to create an intimate contact between plies. The same procedure is repeated until the desired number of plies is stacked. A detailed review on the different heat sources and rollers is given in [16].

ATP can be subdivided in Automatic Tape Laying (ATL) and Automatic Fiber Placement (AFP) which differ by the size of the deposited tapes and the complexity of the stacking. With AFP, the tape has to be unidirectional and small (maximum 1 in. in width) but quite complex curvature components can be manufactured, whereas ATL uses wider tapes (up to 12 in. in width) but enables the stacking of flat laminates only. ATL is therefore faster but the control of the heat is better for AFP because of smaller samples [13,16,42,44].

2.5. Consolidation

A final consolidation step, using a compression press or an autoclave, is generally necessary to reduce the void content of the stacked plies. Porosity (or void content) is indeed another parameter that plays a major role on the composite mechanical properties [45–49]. Voids can be of two origins. The ones within the tapes are called intra-laminar voids and are due to the prepreg fabrication process. Then, when the plies are stacked together, inter-laminar voids appear between individual plies due to ply roughness and imperfect contact (see Fig. 5). It is worth noting that the presence of dissolved moisture in the matrix may

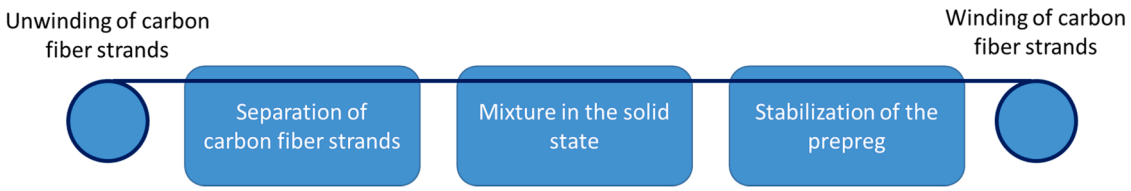

Fig. 3. Scheme of CFRTP prepreg manufacturing process.
Adapted from [37].

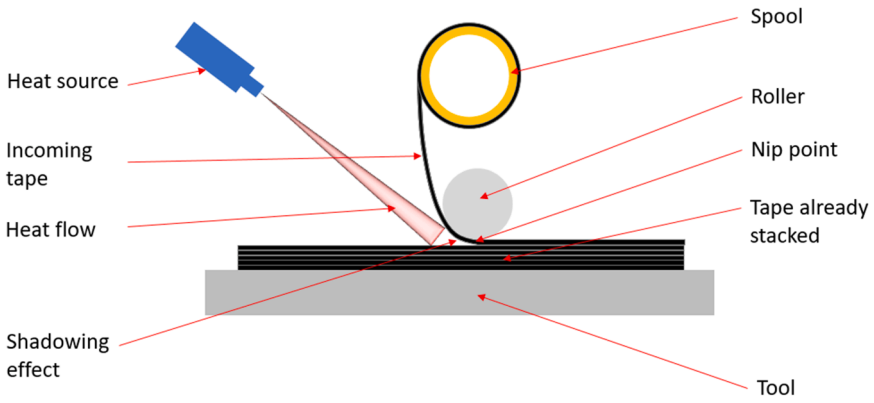

Fig. 4. Scheme of the ATP process.

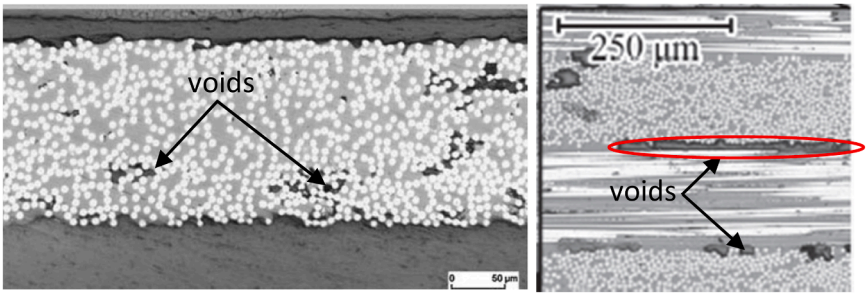

Fig. 5. (a) Cross-sectional optical micrographs to visualize intra-laminar voids (dark spots) of a CF/PEEK tape and (b) Inter-laminar voids of ± 90° stacked CF/PEEK laminates.
(a)Reprinted from Khan et al. [50], ©2010 with permission from John Wiley & Sons (b) Reprinted from Slange et al. [45], ©2018 with permission from Elsevier.

also lead to void formation during consolidation [45]. As the void content increases, the mechanical properties will decrease, so it has to remain below 1% for most aerospace applications [13,14].

With a compression press, a mechanical pressure (often up to 10 bars) is applied on the laminates while controlling the temperature (about 380 °C) and the heating or cooling rate. This process has been widely used in the last decades on CF/PEEK composites for flat geometries [51,52]. Concerning autoclave the sample is placed under vacuum in a vacuum bag, and high temperature is applied for around 1 h along with an additional pressure (6–7 bars) while controlling the heating and/or cooling rate [53–55]. The applied pressure in autoclave enables a very homogeneous distribution of the pressure independently of the part's shape compared to compression press, and composites with quite complex geometries can be consolidated. In both cases, high-quality composites (i.e. with low void content) can be achieved but these routes are costly since high pressure has to be applied for a long time on big volumes (particularly for autoclaves).

Thus, other means to consolidate composites are developed and are known as "out-of-autoclave" processes. The most promising one is the vacuum bagging only (VBO) process [56,57]. As shown in Fig. 6, the laminate is placed under a vacuum bag in an oven under atmospheric pressure. The breather, a porous glass fiber material, homogenizes the vacuum level inside the bag, enabling the application of a pressure close to 1 bar on the laminate. Consolidation occurs when heating above the matrix melting temperature for times similar to those required in autoclaves [56,57]. UD (unidirectional) CF/PEKK laminates with a consolidation level comparable to those via traditional press have already been obtained using this technique [56]. However, the authors point out possible edge and size effects that can arise from this method. Maintaining a homogeneous pressure while having sufficient matrix flow during the consolidation cycle is challenging when the size of specimens increases. Consequently, it may be harder to obtain a homogeneous consolidation quality for large composites.

On-going research aims at developing ATP both for lay-up and "in-situ" consolidation, which would actually be the most interesting solution in terms of productivity [15,18,58,59]. However, the current technological state-of-the-art does not produce yet composites with the same consolidation quality as those obtained by press or autoclave [60].

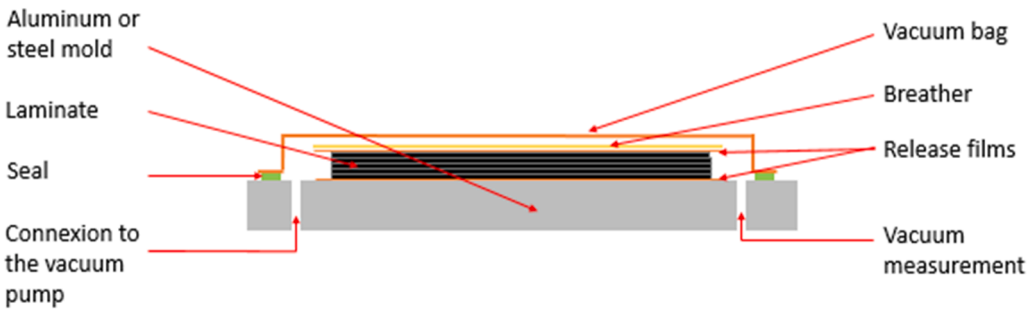

Fig. 6. Schematic representation of the vacuum bagging process.

Though this will be discussed in more details in the last part of this review, a current limit is linked to the high speed of the roller (Fig. 4) causing fast cooling rates and thus low degrees of crystallinity [15,18,58,59,61]. For example, the crystallinity reached for "in-situ" consolidated CF/PAEK through AFP is around 10% as reported in [61] and 18% for CF/PEEK in the study of Comer et al. [55], far below the ones obtained for autoclave processed pieces (see Table 1).

To conclude this part, we summarize in the following table the different processes and associated parameters used in the literature to consolidate CFRTP composites. (Table 2).

3. Rheology of the composite during consolidation

The consolidation step consists in heating and pressing for a few tens of minutes an assembly of plies in order to obtain, as far as possible, a void-free composite. Due to pressure and a temperature above T_m, the matrix and more generally the {fiber + matrix} flow enables the reduction of porosities which can be present within the tape (intra-laminar voids) and between tapes (inter-laminar voids). In this section dedicated to rheology only, the diffusion of volatiles will not be considered (this phenomenon will be discussed in section IV). Hence, the different adhesion mechanisms and flows occurring during consolidation are presented in Fig. 7 for a [0/45] oriented towards y-axis composite. The phenomena have been somewhat arbitrarily divided in two steps. Step 1 concerns phenomena occurring at shorter times whereas Step 2 corresponds to those whose role should mostly influence consolidation at longer times.

The understanding of intimate contact, healing, resin percolation, inter-ply slip, intra-ply shear and squeeze flow, from molecular to macroscopic scale, in such highly-filled systems, is essential to optimize the consolidation process of composites.

3.1. Interfacial adhesion between tapes

During the placement step, the asperities of each ply are brought into contact. These asperities will flatten during consolidation due to temperature and pressure, leading to "intimate contact" as illustrated in Fig. 7.a (IC) [73,74]. Hence, the rougher the surfaces, the longer the time for intimate contact between tapes. When intimate contact is achieved, molecular chain interdiffusion between the upper and lower plies will occur, as shown in Fig. 7.b (H) [75]. This phenomenon, sometimes called healing or autohesion [64], will reduce the amount of inter-laminar voids. Inter-laminar bonds between individual plies will then lead to the development of inter-laminar strength [50,74,76,77]. Avenet et al. [64] studied the development of bonding strength on CF/PEKK composites at short processing times. They outlined the role of

Table 2
Processing parameters according to the manufacturing process and materials.

Process	Placement speed (m/min)	Tool temperature (°C)	Processing temperature (°C)	Pressure and/or *Applied force*	Heating rates (°C/min)	Cooling rates (°C/min)	Dwell time (min)	Material	References
Autoclave	/	/	380	7 bar	3	2	45	CF/	[50]
	/	/	375	7 bar	3	2	20	PEEK	[55,62]
	/	/	390	7 bar + 1 bar	5	5	30		[63]
	/	/	390	3–20 bar	15	10–15	30		[53]
	/	/	350–400	3–10 bar	3	10	15–30–45		[54]
	/	/	380	?	?	?	120	CF/ PEKK	[64]
Hot Press	/	/	330	5–17 bar	7–10	2–3	15–30	CF/PPS	[65]
	/	/	400	3–10 bar	?	18	30–120	CF/	[51]
	/	/	400	7 bar	2	2	15	PEEK	[66]
	/	/	380	40 bar	3	16	10	CF/ PEKK	[60]
VBO	/	/	380	~1 bar	2.8	2.8	0	CF/	[67]
	/	/	400	0.9 bar	2	2	15	PEEK	[66]
	/	/	360	0.3–1 bar	5–20	0.5–10	15	CF/	[56,68]
	/	/	375	0.9–1 bar	4–5	?	30	PEKK	[69]
	/	/	380	0.95 bar	3	7	30		[60]
AFP in-situ	3–9	300	?	*50–225 N*	/	/	/	CF/	[50]
	3	Unheated	380	2.5 bar	/	/	/	PEEK	[70]
	9	Unheated	420	3.8 bar *(365 N)*	/	/	/		[71]
	8	150	1350 W = 420 °C	1.2 bar	/	/	/		[55,62]
	5–9	280	HGT (800–1300 °C)	*100–200 N*	/	/	/		[72]
	3	?	HGT 910 °C	*355 N*	/	/	/		[63]
	2.4–6	?	3400 W (~417–430 °C)	*1000 N*	/	/	/		[60]
	2	200	180 W	~20 bar *(500 N)*	/	/	/	CF/ PEKK	[66]

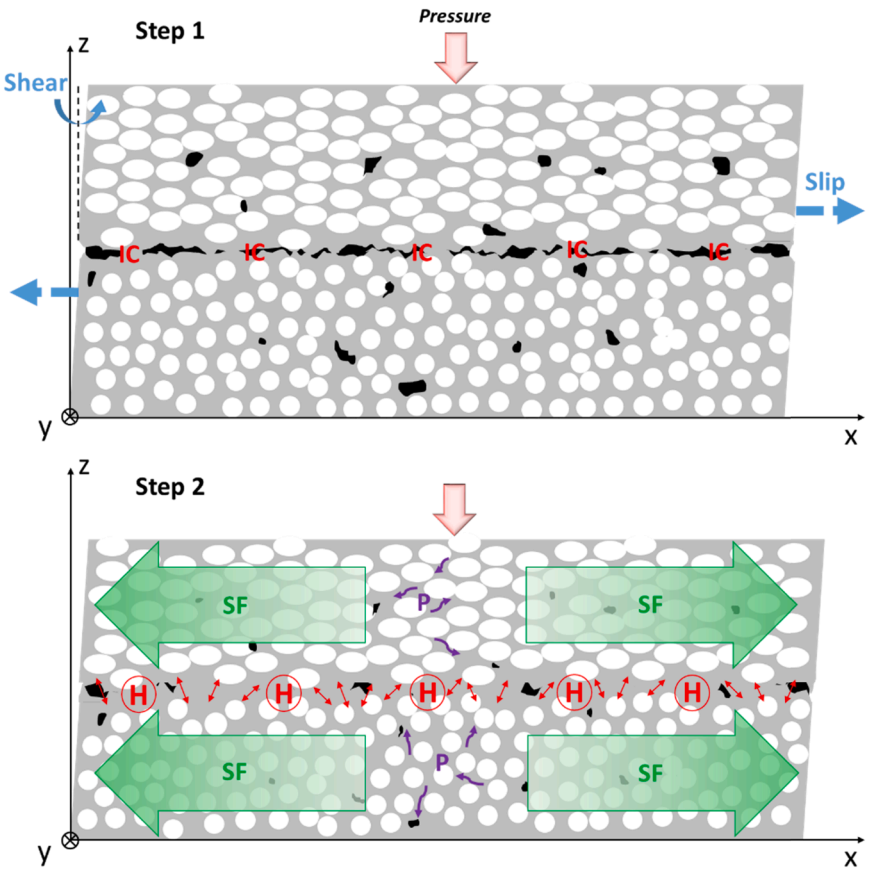

Fig. 7. Schematic illustration of the different phenomena occurring during consolidation of a [0/45] oriented towards y-axis. The matrix is represented in grey color. White ellipses stand for the 45° oriented fibers and white circles for the 0 ° oriented fibers. Voids (in black) can be present within a ply (intra-laminar void) or at the interface between plies (inter-laminar voids). Step 1: "IC": intimate contact development, "Slip": inter-ply slip, "Shear": transverse intra-ply shear; Step 2: "H": healing, with red arrows representing chain interdiffusion, "P": resin percolation, "SF": squeeze flow.

fibers on the bonding strength, especially confinement effects on the matrix due to the high volume fraction of fibers. Besides the regimes corresponding to intimate contact and healing development, it is worth pointing out they identified a third regime corresponding to fiber bridging, i.e. the formation of a continuous fibers path which leads to a further increase in the bonding strength. This suggests presence of fibers will lead to a stronger interface between tapes than if filled with resin only.

Depending on the pressure and temperature applied during the consolidation cycle and also on the initial roughness, either intimate contact or chain interdiffusion can take more time to occur [57,75]. While the typical time for chain interdiffusion is related to the reptation time, on the order of 10–100 s at the processing temperatures, intimate contact times can vary between about 1 s and 1 h depending on the initial roughness [75]. Concerning pressure, a threshold value of 1 MPa (10 bar) has been estimated for CF/PEEK [78,79] above which the characteristic intimate contact time becomes lower than the time required for healing. However, in the VBO process, the pressure applied on the samples is low, typically 0.1 MPa (1 bar), hence this part of the consolidation, consisting in lowering the voids and ensure the adhesion between tapes, will be mainly governed by the characteristic time for intimate contact (100 – 1000 s) [75]. Despite the high pressure applied, one of the main issues in achieving "in-situ" consolidation is indeed the time spent above T_m (< 1 s [77]), shorter than the time needed for healing. Butler et al. [80] developed a coupled bonding model introducing a non-dimensional parameter related to the ratio between the two characteristic times to determine which of the intimate contact or healing phenomenon shall be preponderant. This may be helpful in cases both timescales are similar, for example when bonding smooth surfaces with a low pressure, such as in VBO consolidation.

As stated previously, chain interdiffusion only occurs after intimate contact is achieved. It is therefore fundamental to optimize intimate contact during tape placement and consolidation. The degree of intimate contact D_{ic} is defined as the ratio between the surface area in contact and the surface of the tapes assuming perfectly flat surfaces [50,57] and often used to estimate its quality. During consolidation, D_{ic} increases. However, intimate contact only occurs in resin-rich regions. Indeed, portions of the ply surface may consist in dry fibers where no bonds with the neighboring tape will develop. Celik et al. [73,81] then introduced the concept of *effective* intimate contact which corresponds to the ratio between the surface of the resin-rich surface (i.e. from which dry areas were removed) and the total surface of the tapes.

Many models describing the evolution of the asperities and thus the variation of D_{ic} during intimate contact exist and are discussed in [57,75]. Yang et al. [74,79] defined a model using Cantor fractal-shaped asperities corresponding to the Fourier transformation of experimental observations. This model describes well uncharged or low-filled polymers but since the carbon fiber volume fraction is close to 60% in unidirectional CF/PAEK composites, the effect of fibers on asperities deformation should be considered. This has been done by Levy et al. [82] with a finite element analysis, showing that adhesion takes place first at the edges of the contact area and then extends progressively to the whole contact area.

3.2. Flow mechanisms during consolidation

Four flow mechanisms are generally identified during consolidation: inter-ply slip (Fig. 7.a (Slip)), intra-ply shear (Fig. 7.a (Shear)), matrix percolation (Fig. 7.b (P)) and squeeze flow (Fig. 7.b (SF)) [57]. Another flow mechanism, elongational deformation, will not be detailed further in the following, as it can be considered negligible for continuous CFRTP. Compression is the main solicitation during consolidation, and elongational viscosity is known to be extremely high for continuous CFRTP [83,84].

3.2.1. Matrix percolation

Matrix percolation refers here to the microscopic flow of the matrix through the fiber network within a ply [85]. This local redistribution of resin is a similar mechanism to the one responsible for healing between plies [85]. However, and contrary to thermosets [86] (viscosities in the 1–10 Pa.s range [8]), the viscosity of thermoplastics is generally high at the processing temperature (100–1000 Pa.s [87]). For CFRTP with a fiber volume fraction close to 60%, the fibers are highly packed and thus, percolation through the fiber network will occur over times much higher than the other flow mechanisms [85].

3.2.2. Inter-ply slip

Inter-ply slip is the translational movement of one ply relative to the others (Fig. 7.a (Slip)). Cogswell et al. [88] showed that such slip is more important when the plies are stacked with different orientations because of thicker resin-rich areas at the interface, easing the inter-ply slip while reducing fiber-fiber friction [85,88,89]. This type of deformation is therefore only dependent on the shear viscosity of the neat matrix [85]. For CF/PEEK laminates, Cogswell et al. [88] also showed that there is a yield stress (> 100 Pa) before the plies start to slide and then that sliding velocity is proportional to the applied shear stress. Kaprielian et al. [89] noted that there is no possible rotation of the layers between themselves. Further measurement of the shear stresses involved during consolidation is still needed to conclude about such sliding of plies but due to low forces applied in OOA consolidation and high viscosities, inter-ply slip shall remain limited.

3.2.3. Intra-ply shear

Intra-ply shear defines the shearing process of the whole {matrix + fibers} system within the ply (Fig. 7.a (Shear)). Shear can be parallel to the fibers (Υ_L, "axial - or longitudinal - intra-ply shearing") or perpendicular to the fibers (Υ_T, "transverse intra-ply shearing") [57,90]. Shearing occurring during compression will affect the rheology of the system.

3.2.3.1. Rheological measurements settings. It is relatively well-known that PAEK polymers, like many other thermoplastics, behave as Newtonian fluids at low shear stresses and as shear thinning fluids at high shear stresses [35,91,92]. However, the rheological characterization of reinforced polymers is more complex and specific experimental set-ups have then to be designed.

UD tapes are inherently anisotropic, meaning their macroscopic rheological response is different along the fibers and transverse to the fibers. Many authors agree that there is no flow of the resin along the fibers. As stated previously, Goshawk et al. [93] explain that the effective viscosity in the fiber direction is much higher than the one in the transverse direction due to fibers' inextensibility [94].

Groves et al. [95] first measured the rheological properties of cross-ply CF/PEEK composites, both under oscillation and in the steady-state shear. They obtained the "isotropic" viscosity of the composite, which corresponds to the macroscopic viscosity of the sample under shear.

A less simplistic approach was developed by Rogers et al. [96] who obtained the analytical relations to decouple the longitudinal and transverse components of the viscosity. Their approach is based on the expression of the torque M of an elastic response:

$$\boldsymbol{M}\cdot\boldsymbol{H} = (\boldsymbol{G_T}\cdot\boldsymbol{I_T} + \boldsymbol{G_L}\cdot\boldsymbol{I_L})\cdot\boldsymbol{\theta} \tag{1}$$

where G and I are the shear moduli and the second moments of area (or moments of inertia) respectively, in the transverse ($_T$) and longitudinal ($_L$) directions, Θ is the amplitude of the twist angle and H the distance between plates.

In order to obtain both longitudinal and transverse components of the viscosity, different second moments of area along the fibers and transverse to the fibers are needed, i.e. $I_T \neq I_L$. This can be obtained either by cutting rectangular specimens (with different aspect ratios) or by placing two off-centered specimens as shown in Fig. 8.

For a viscoelastic material, the rheological parameters such as the moduli, the torque or the twist angle are time dependent. Eq. (1) can then be decomposed in Eqs. (2 and 3) [91] (for more calculation details, refer to [96]):

$$\boldsymbol{M_0}\cdot\boldsymbol{H}\cdot\boldsymbol{cos}(\boldsymbol{\delta}) = (\boldsymbol{I_T}\cdot\boldsymbol{G'}_T + \boldsymbol{I_L}\cdot\boldsymbol{G'}_L)\cdot\boldsymbol{\theta} \tag{2}$$

$$\boldsymbol{M_0}\cdot\boldsymbol{H}\cdot\boldsymbol{sin}(\boldsymbol{\delta}) = (\boldsymbol{I_T}\cdot\boldsymbol{G''}_T + \boldsymbol{I_L}\cdot\boldsymbol{G''}_L)\cdot\boldsymbol{\theta} \tag{3}$$

where M_0 is the amplitude of the torque, δ is the phase angle, G'_T (G'_L) and G''_T (G''_L) are respectively the storage and loss moduli in the direction transverse (resp. longitudinal) to the fibers.

Recently, Deignan et al. [91] modified again the geometry of the specimens by cutting rectangles with lengths much longer than their widths to have $I_T >> I_L$ and measure only the transverse component of the viscosity. In this study, the authors specifically worked on single plies in order to avoid inter-ply slip, which might play a role in the rheological measurements presented previously. It is quite important to be able to dissociate inter-ply slip and intra-ply shear in order to get the transverse viscosity of the composite. This viscosity as a function of the angular frequency ω can be obtained from the measurements of the transverse storage and loss moduli, as given by Eq. (4):

$$\boldsymbol{G'}_T = \left(\frac{\boldsymbol{H}\cdot\boldsymbol{M}}{\boldsymbol{I_T}\cdot\boldsymbol{\theta}}\right)\cdot\boldsymbol{cos}(\boldsymbol{\delta})$$

$$\boldsymbol{G''}_T = \left(\frac{\boldsymbol{H}\cdot\boldsymbol{M}}{\boldsymbol{I_T}\cdot\boldsymbol{\theta}}\right)\cdot\boldsymbol{sin}(\boldsymbol{\delta}) \tag{4}$$

$$\boldsymbol{\eta_T} = \frac{\sqrt{\mathbf{G'}_T^{\,2} + \mathbf{G''}_T^{\,2}}}{\boldsymbol{\omega}}$$

Another intra-ply rheological characterization has been described by Stanley et al. in [94]. It consists in using a rheometer with three plates: the upper and lower ones are fixed while the middle plate is pulled-out at a constant speed or force (see Fig. 9). Two samples are therefore considered: one between the upper and the middle plates and another between the middle and the lower plates. This configuration generates a shear on the two tested samples, with different rheological responses depending on the fiber orientation with respect to the pullout direction.

In order to avoid inter-ply slip, the samples are rotated such that the interlayers (shown by the red dashed lines in Fig. 9) are perpendicular to the pullout direction. The upper sample has fibers oriented along the pull-out direction, hence longitudinal shear occurs. The lower one has fibers perpendicular to the pull-out direction, hence transverse shear occurs.

Haanappel et al. [90,98], developed a torsion bar test adapted on a rheometer with the specimen fixed at each side of its cross section (Fig. 10) to calculate the longitudinal shear viscosity. The upper part rotates while the lower one remains static, leading to a deformation in torsion. The fibers direction is normal to the shearing direction, in order to prevent the specimen from inter-ply slip.

3.2.3.2. Rheological characterization. In [97,99], Groves et al. used off-centered square samples described in Fig. 8 to separate the longitudinal and transverse components of the complex viscosity and were then the first to measure properly the transverse viscosity of CF/PEEK composites. They evidenced a yield stress fluid behavior, such as the viscosity follows (Eq. 5):

$$\boldsymbol{\eta} = \boldsymbol{m}\dot{\boldsymbol{\gamma}}^{\boldsymbol{n-1}} \tag{5}$$

with m and n the parameters of the power-law viscosity, $\dot{\gamma}$ the shear rate.

They obtain m close to 10^5 Pa.s^n and n close to 0 at 380 °C for the transverse viscosity.

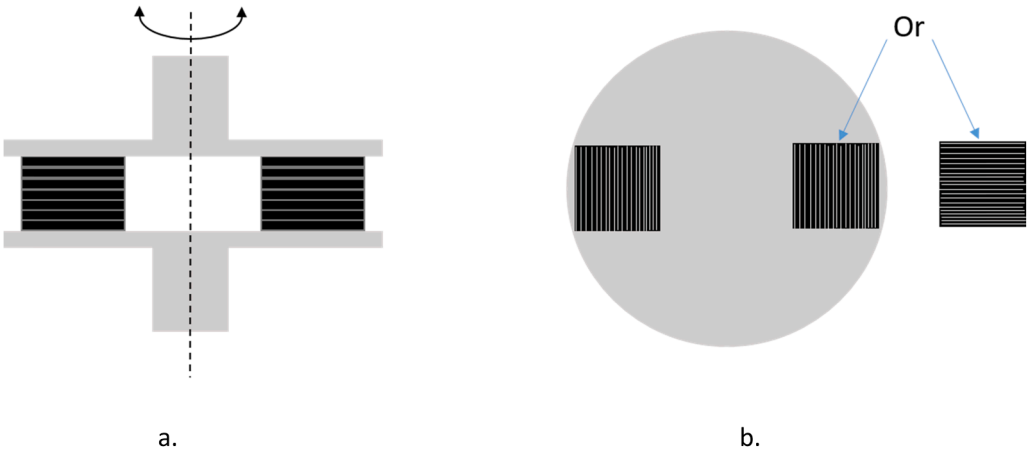

Fig. 8. Schematic representation of complex viscosity measurement of an anisotropic material using a plate-plate rheometer (a: side view; b: top view). Adapted from [97].

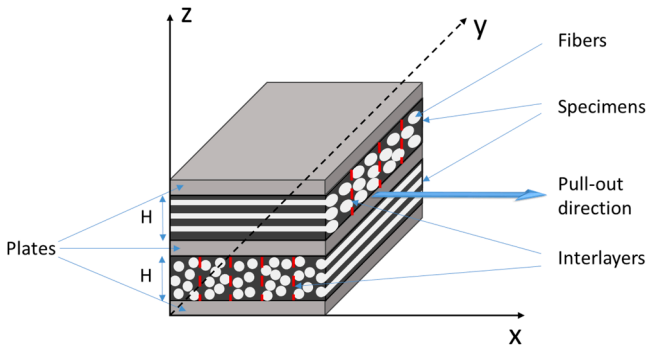

Fig. 9. Schematic representation of the intra-ply shear characterization setup Adapted from [94].

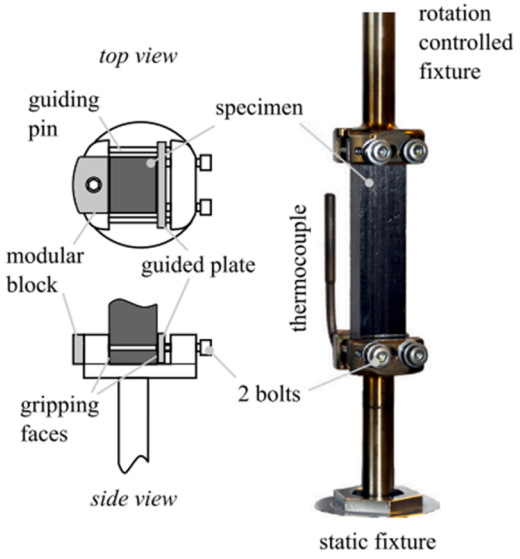

Fig. 10. Schematic representation of the torsion bar test.
Reprinted from Haanappel et al. [90], ©2014 with permission from Elsevier.

According to Deignan et al. [91,100], CF/PEEK composite also behaves as a yield stress fluid at low shear rates with a pseudo-elastic behavior governed by fiber-fiber friction, and a shear-thinning behavior at all measurable frequencies (see Fig. 11.a). From Fig. 11.a and assuming the Cox-Merz rule is valid (i.e. $|\eta^*(\omega)| = \eta(\dot{\gamma})$), which has not been clearly evidenced for composites [74], values of 10^5 Pa.s^n and close to 0 for m and n respectively (see Eq. 6) can be extracted for the transverse viscosity at the same temperature as Groves, using a similar approach. At very high shear rates ($> 10^3$ s^{-1}), the viscosity of the composite shall be the one of the matrix [91,100]. This phenomenon has also been observed on short-carbon-fiber-reinforced PEKK by Kishore et al. [92].

Using the set-up presented in Fig. 9, Stanley et al. also characterized a shear thinning behavior CF/PEEK composites [77]. However, they obtained m and n values of 7.10^3 Pa.s^n and 0.2 respectively, again at 380 °C.

If the different viscosity measurement tests presented in this section differ from each other and require quite complex settings, all demonstrate that CF/PAEK composites behave as a shear thinning fluid with high-level of viscosities in the range of frequencies studied. We want to highlight again that the values obtained for m and n can differ depending on the experimental set-up chosen. Inter-ply slip may explain a decrease in the "apparent" viscosity measured by Stanley [77] compared to Groves [82] and Deignan [74], but this confirms robust measurements of such composite viscosity are still needed (see also section II.2.4).

Note that Haanappel et al. [90] also described a shear thinning behavior for the longitudinal viscosity, with $m \approx 10^7$ Pa.s^n and $n \approx 0$ at 390 °C. Comparing these results to the ones discussed above is consistent with experiments by Goshawk et al. [93] suggesting longitudinal viscosity is much higher than the transverse one.

3.2.3.3. Effect of pressure and temperature on CFRTP viscosity. Fig. 11.a also highlights the effect of pressure on the rheological behavior of a composite. The values of viscosities increase by almost an order of magnitude when the applied pressure increases from 52 kPa to 313 kPa. This is due to an additional phenomenon called shear-banding which appear during the rheological test. Shear-banding occurs when only a small portion of the ply (~ 10% of its thickness) is in motion (i.e. flows) while the rest remains in a "solid" state [101]. As illustrated in Fig. 11.b, when shear-banding occurs, the deformation through the sample is not homogeneous. This situation is then in contradiction with the fact that during a rheological test, homogeneous deformation within the sample is assumed.

This has been confirmed on CF/PEEK composites by Deignan et al. [91] by measuring the complex viscosity of a single ply (to avoid inter-ply slip during the experiment) for different pressures, as shown in Fig. 11.b. If the pressure applied is too low, shear-banding results in a partial flow only, and thus to a measured viscosity much smaller than expected. When the pressure is high enough, shear-banding is suppressed, the measured viscosity increases significantly and becomes independent of the pressure applied.

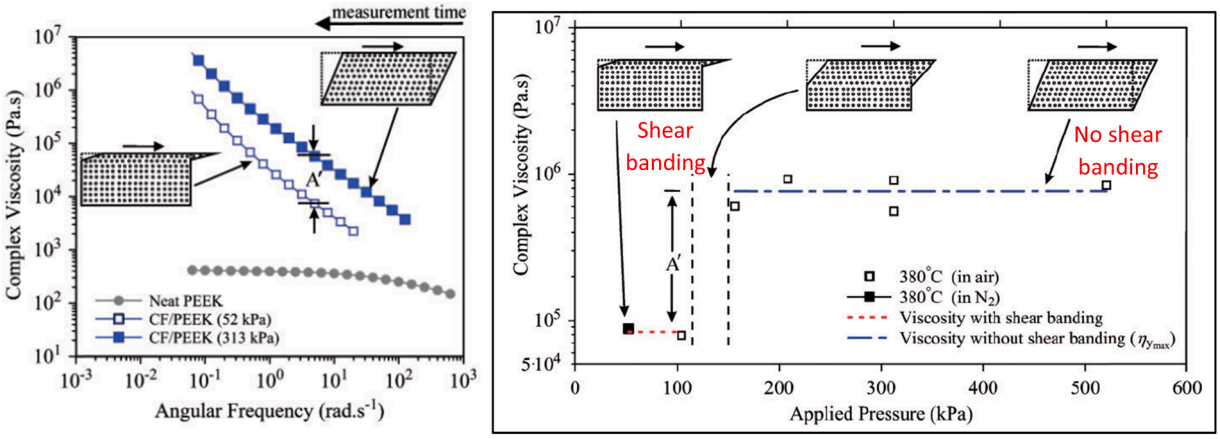

Fig. 11. a. Angular frequency sweep of a CF/PEEK single-ply at 5% strain and at 380 °C in air and b. Complex viscosity as a function of the applied pressures. Reprinted from Deignan et al. [91], ©2018 with permission from SAGE.

Finally, we shall mention the effect of temperature on CFRTP viscosity measurements is not clear. The high fiber volume fraction may explain why the viscosity of the CF/PEEK does not depend much on the temperature [90,98]. It is worth mentioning that an increase in viscosity with temperature is evidenced in [91]. It might be due to the fact that in this study, the rheological tests were conducted under high pressure. Hence, the material is compressed during the whole measurement, which can lead to an increase in fiber volume fraction during the experiment due to flowing of the matrix out of the testing area. This compression is more pronounced at higher temperatures as the viscosity of the matrix decreases with temperature. As the fiber-fiber friction hampers the flow of the matrix, the "apparent" viscosity of the composite may then increase with temperature when high pressure is applied. An optimum between pressure and temperature may therefore be conceivable.

3.2.4. *Squeeze flow*

Squeeze flow (Fig. 7.b (SF)) is the radial flow occurring when the composite is subjected to axial compression. A schematic representation is presented in Fig. 12 for a disk-shaped sample. During consolidation, squeeze flow will redistribute fiber and matrix within a ply and should be the main mechanism for intra-ply voids reduction, as reported by Shuler et al. [102]. Squeeze flow depends on pressure, temperature and time. Note that, a priori, there is no such radial flow at the center of the composite (dark red circle in Fig. 12.a) so that in this region the reduction of porosity originates from another mechanisms, such as slow resin percolation (see Fig. 7.b) [85].

Squeeze flow can be characterized by two different rheological tests. Either the force is fixed and the gap displacement is measured as a function of time, or the squeeze rate (closure speed of the plates) is fixed and the force required to maintain this speed is recorded as a function of gap displacement [102,103]. The sample surface can have the same surface as the plates, leading to a constant surface under compression all along the experiment (Fig. 12.a). Alternatively, the samples can have a surface much smaller than the plates such that the volume of the sample between the plates remains constant during the experiment (Fig. 12.b).

3.2.4.1. Modelling squeeze flow for neat polymers. Squeeze flow models are well known and the most common one, established for Newtonian fluids, is known as the Stefan's law [104]. When the surface between plates remains constant (Fig. 12.a), it can be written for a disk as Eq. (6):

$$F = 3\pi R^4 \eta \frac{-\dot{h}}{8h^3} \tag{6}$$

where F is the applied force, R the radius of the plates, η the viscosity of the fluid, h the half gap (see Fig. 12.a) and $\dot{h}$ the squeeze rate.

The hypotheses behind the Stefan's law are the following: the inertial and gravity terms are neglected, the specimen is in steady-state regime, a no-slip condition is assumed between the sample and the plate, and the

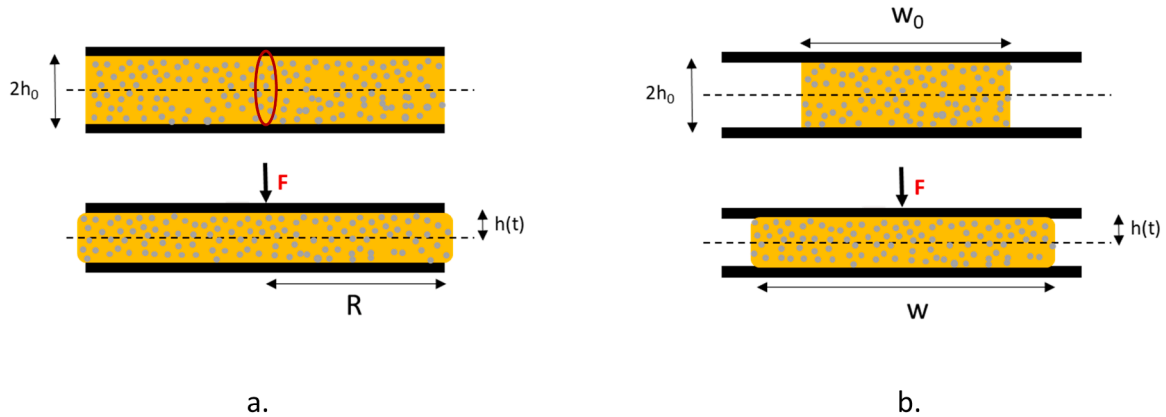

Fig. 12. Schematic representation of a specimen squeezed between two parallel plates (a) in a " constant surface " configuration and (b) in a "constant volume" configuration.

fluid fills entirely the gap.

Many extensions of this model exist and have been reviewed by Leider et al. [105]. One of these extensions, Scott's law [106], is of particular interest in the case of CF/PAEK composites, recalling the discussion of the previous section. It generalizes Stefan's law solution for a fluid having a power law viscosity, in the case of constant surface (Eq. 7):

$$F = \frac{\left(-\dot{h}\right)^n}{h^{2n+1}}\left(\frac{2n+1}{2n}\right)^n \frac{\pi m R^{n+3}}{n+3} \tag{7}$$

Jackson et al. [107] used Eq. (7) under a constant closing speed and highlighted a size effect on the ease of squeezing. They determined that the higher the ratio between the length and the thickness, the harder the squeezing. This might be an issue on consolidation suggesting that it may become harder to reduce porosities thanks to squeeze flow when the size of the sample increases.

3.2.4.2. Modelling squeeze flow for fiber-reinforced thermoplastics. Thattaiparthasarthy et al. [103] used Scott's equation on polypropylene filled at 40% in volume by discrete long (~ cm) glass fibers, considering the fluid as an isotropic, non-Newtonian, power-law type fluid under isothermal conditions. The isotropic hypothesis is assumed because the shape of the specimen remained circular after the squeeze flow experiment. They obtained shear power-law parameters m close to 2.10^4 Pa.s^n and n in the 0.35–0.4 range at 190 °C.

Stefan's and Scott's solutions have also been used to model the experimental results obtained for the squeeze flow of continuous fiber reinforced thermoplastic composites. However, the presence of continuous fibers seems to render the isotropic continuum hypothesis incorrect [93]. Assuming the velocity is equal to 0 along the fiber, i.e. flow occurs only perpendicular to the fibers, Rogers et al. [108] proposed a first approach based on a Newtonian fluid under a constant normal force which does not consider the shear-thinning behavior observed for these composites. Assuming no-slip and a constant volume, the gap evolution with time is given by Eq. (8):

$$F = -2\eta L \frac{\dot{h}}{h^6}(w_0 h_0)^3 \tag{8}$$

where w_0 the initial half width of the specimen (see Fig. 12.a), L the length, η the apparent viscosity of the whole {matrix + fibers} system.

As stated, this model cannot fully predict the experimental squeeze flow for CF/PAEK composites since it totally neglects the characteristic shear-thinning behavior discussed in the previous section.

The authors want therefore to highlight an analytical solution developed by Advani et al. [109] that models the squeeze flow of CFRTP on square plates, taking into account both the anisotropy of the {fiber + matrix} flow and the power-law type profile of the viscosity (see Eq. 5). The solution is given in Eq. (9) in the case of constant volume for a rectangular sample:

$$F = \frac{\left(-\dot{h}\right)^n}{h^{2n+1}}\left(\frac{2n+1}{n}\right)^n \frac{2m}{n+2} L w^{n+2} \tag{9}$$

where w and L are the half-width and length of the sample respectively (see Fig. 12).

Numerical attempts have also been conducted to model the squeeze flow behavior of CFRTP. Shuler et al. [102] used a cell model where a single fiber is surrounded by an incompressible matrix fluid. Wang et al. [110] took into account the viscosity increase during the squeeze flow, due to the "locking" of fibers (i.e. the composite becoming harder to compress as the fiber volume fraction increases) [57,111,112]. Goshawk et al. [93] developed a two-dimensional finite element model where the material is composed of non-deformable fibers and a Newtonian fluid. Such numerical models usually simulate satisfyingly experimental data at short times but deviations occur at longer ones, due to effects such as fiber displacement during squeeze flow or shear-thinning of the matrix.

3.2.4.3. Squeeze flow experiments: an original method to determine the viscosity of a composite. Through Stefan's law extensions presented in the previous part, some authors have also used squeeze flow experiments as an indirect method to obtain more easily the viscosity of a CFRTP composite than with the methods presented in II.2.3. It might also provide a more useful information as it gives directly access to the steady shear viscosity rather than the complex viscosity. However, most authors used the model developed by Rogers [108] for Newtonian fluids and determined the transverse shear viscosity of a UD composite by deriving Eq. (8) [50,57,109,113]:

$$\eta_T = \frac{5}{2}\frac{Ft}{L_0 w_0^3}\frac{h_0^2 h^5}{h_0^5 - h^5} \tag{10}$$

where η_T is the transverse viscosity of the system {matrix + fibers} and L_0 and w_0 the initial length and half-width of the sample respectively.

To the best of the authors' knowledge, none of the viscosity estimates through squeeze flow experiments have been done using Eq. (9) or any model considering both flow anisotropy and a power-law viscosity, which could then be the aim of future work.

Saffar [57] used Eq. (10) to fit experimental data of unidirectional CF/PEKK squeeze flow and obtains a constant transverse viscosity of about 10^6 Pa.s. This value is in the same range as those measured by Deignan et al. [91,100] for CF/PEEK composites (see Fig. 11.a) but obviously do not capture shear-thinning.

To go beyond, Saffar [57] re-estimated the apparent transverse viscosity η_{T0} of UD CF/PEKK composites applying a Carreau-type law for the fluid (Eq. 11):

$$\eta_T(\dot{\gamma}) = \eta_{T0}\left[1 + (\lambda\dot{\gamma})^2\right]^{\frac{n-1}{2}} \tag{11}$$

where η_{T0} is the zero-shear transverse viscosity, λ the relaxation time and n as defined in Eq. (6).

Zero-shear viscosity around 10^9 Pa.s and n close to 0,05 were obtained at 380 °C, both far from values typically measured in the literature for these materials [91,100,102]. Nevertheless, as suggested by Deignan, CF/PEEK shall have a yield stress fluid-like behavior [91,100]. Hence, the use of a Carreau-fluid law to describe the composite behavior may not be appropriate. Still, estimating the viscosity at 1 s^{-1} with the parameters of this Carreau-law, we obtain a value around 3.10^3 Pa.s for m, much smaller than the values obtained by Groves [82] and Deignan [74] (see section II.2.3).

To sum up, the squeeze flow of neat polymers is well-modeled by existing analytical developments. However, despite numerous models (analytical or numerical) that have been developed to describe the rheological behavior of composites, a full-agreement between theory and experimental data concerning squeezing of a CFRTP has still not been reached. A direct link between squeeze flow and intra-ply void reduction over time to evaluate its impact on the consolidation quality is also lacking. Wang et al. [20] suggest that the future squeeze flow models should be fully predictive and physical (i.e. not semi-empirical). To do so, they shall be rate and temperature dependent, consider non-Newtonian effects and the elastic contribution of the fibers as well as the fiber rearrangement during shearing.

We also want to underline that all the squeeze flow models used for composites consider no-slip boundary conditions, a hypothesis often not really justified. Yet, it has been demonstrated that slip may exist between neat polymers and plates even at relatively low shear rates (~ 1 s^{-1}), which can significantly affect the viscosity measurement [114,115]. A proper characterization of slip between CRFTP and plates is then important to incorporate correct boundary conditions in the squeeze flow models [116], but such experiments have not been performed to the best of our knowledge. Hatzikiriakos et al. [117] describe various

strategies to measure slip in neat polymers, which may be adapted to composites.

4. Consolidation quality improvement

Nowadays, consolidation on thermoset-based composites are quite well-mastered and can even be modelled efficiently [118,119]. Consolidation of thermoplastic-based composites is more complicated because of higher viscosities (100–1000 Pa.s [87] compared to 1–10 Pa. s for thermosets [8]) and processing temperatures (380 °C versus typically 180 °C for a CF/epoxy composite [120]). Table 3 summarizes the microstructural characterization and mechanical properties found in the literature for different processes and materials. Most of the results presented in the table will be discussed in further details in this section. Thus, this last section aims at reporting different options discussed in the literature to improve the final consolidation quality of a CF/PAEK composites.

4.1. Optimization of the tape

During both the lay-up and the consolidation step, the matrix must flow and fill-in as much as possible pre-existing porosities during the cycle time. This flow is eased when the pressure and/or the temperature are high. For a combination of rapid lay-up (AFP) followed by OOA consolidation (where low pressure is applied), it is essential to optimize the architecture of the tape, i.e. fiber-matrix distribution (fibers repartition, presence of resin-rich regions at the surface), distribution of the porosities, and surface roughness.

Many authors [50,123,124] insist on the importance of obtaining a tape homogeneous in thickness (low roughness), with a good fiber-matrix distribution and a low-void content. A good dispersion of the fibers within the matrix prevents from void creation through matrix cracking or fiber-matrix debonding [123]. Smooth tapes favor intimate contact (D_{ic}) and then chain interdiffusion between tapes, leading to inter-laminar void reduction [50]. Still, Centea et al. [125] recently highlighted the work of Thorfinnson [126], suggesting rather counter-intuitively that prepregs with high initial void content due to areas not wet by the matrix may facilitate the evacuation of moisture and other volatiles before being entrapped by the resin. However, dry areas will also lead to local fibers concentrations that may prevent the matrix from flowing and filling in these voids during consolidation. This is even more true for highly viscous resins consolidated under low pressures, for example with the VBO process. This suggests the existence of an optimum depending on the final process used.

The presence of resin-rich regions at the surface of the tape also seems an interesting strategy to increase the consolidation quality [123, 127,128]. Sacchetti et al. [127] estimated the fracture toughness of CF/PEEK composites with different matrix interleave thicknesses through G_{IC} measurements. The thicker the resin interlayer, the higher the fracture toughness of the composite, as intimate contact and chain interdiffusion is favored at the interface. When the interlayer thickness increases, the plastic yield zone increases, meaning that more energy is dissipated and hence higher mechanical properties at the tapes' interfaces can be achieved [127]. Obviously, a balance between this interlayer thickness and the final fiber content in the composite shall be observed. Sacchetti et al. [127] also concluded that migration of fibers at the tapes' interface does not increase the fracture toughness of the CF/PEEK composite, in contradiction with Avenet et al. [64] who attributed an increase in G_{IC} on CF/PEKK for longer welding times to fiber bridging.

Following a similar approach, Slange et al. [123] studied the effect of tape architecture and lay-up quality on the final consolidation quality. Two different CF/PEEK tapes were placed by ultrasonic welding, AFP or press and then stamp formed. The so-called "void free" [123] TC (TenCate, USA) tape has a smooth surface with a good fiber-matrix repartition but with no matrix layer at the interface (as shown in Fig. 13.a). CY (Cytec, USA) tape has a non-uniform thickness and a high void content (around 5–10%) but displays matrix-rich regions (see Fig. 13.b). The void content is characterized by a non-destructive technique based on ultrasonic transmission (US C-scan measurements). US C-scans in Fig. 13.c-d show a better consolidation quality for CY-tape based composites (void content around 0.5% for CY laminates against 1.3% for TC laminates), which can be explained by the fact that the resin-rich regions, despite the rougher surfaces, lead to better inter-laminar bonding

Table 3
Microstructural and mechanical properties for different processes and materials.

Process	Orientation	Material	Degree of crystallinity (%)	Porosity rate (%)	ILSS (MPa)	Flexural strength (MPa)	References
Autoclave	?	CF/PEEK	/	/	94	/	[50]
	$[0]_{16}$		25	2.8	105	/	[70]
	$[+45/-45]_{4s}$				41		
	$[0]_8$		35	?	/	1650	[71]
	$[0]_{30}$		42	/	/	/	[62]
	$[0]_{16}$		> 40	< 0.1	110	1600	[55]
	$[0]_{24}$		36	0.03	/	/	[63]
	$[0]_{16}$		/	< 1	120	/	[53]
	$[0/90]_{4s}$			1–1.4	100		
Hot Press	?	CF/PEEK	30–40	/	/	/	[51]
	$[0]_{16}$		43	0.4–0.9	109	1856	[66]
	$[45/0/-45/0/90/45/-45/90]_s$	CF/PEKK	19–21	< 0.5	90–95	/	[60]
VBO	$[0]_{16}$	CF/PEEK	40	0.8–1.2	107	1812	[66]
	$[0]_{16}$	CF/PEKK	/	/	60–100	/	[56,68]
	$[45/0/-45/0/90/45/-45/90]_s$		18–22	1–3	50–70	/	[60]
	$[(0_4/90_4)_40_4]_s$			0.6–3.8			[67]
AFP in-situ	$[0]_{16}$	CF/PPS	16–29	/	45	/	[121]
	$[0]_{16}$	CF/PEEK	/	1.5–3.5	40–80	/	[50,72]
	$[0]_{16}$		25	3.4–4.2	45	/	[70]
	$[+45/-45]_{4s}$				20		
	$[0]_8$		17	5.2	/	1143	[71]
	$[0]_{30}$		18	/	/	/	[62]
	$[0]_{16}$		/	2.8	80	1300	[55]
	$[0]_{24}$		23.7–30.4	0.23–0.42	/	/	[63]
	$[0]_{16}$		/	1.5	/	/	[122]
	$[0]_{16}$		37	3	71	1505	[66]
	$[45/0/-45/0/90/45/-45/90]_s$	CF/PEKK	3	6–7	20	/	[60]

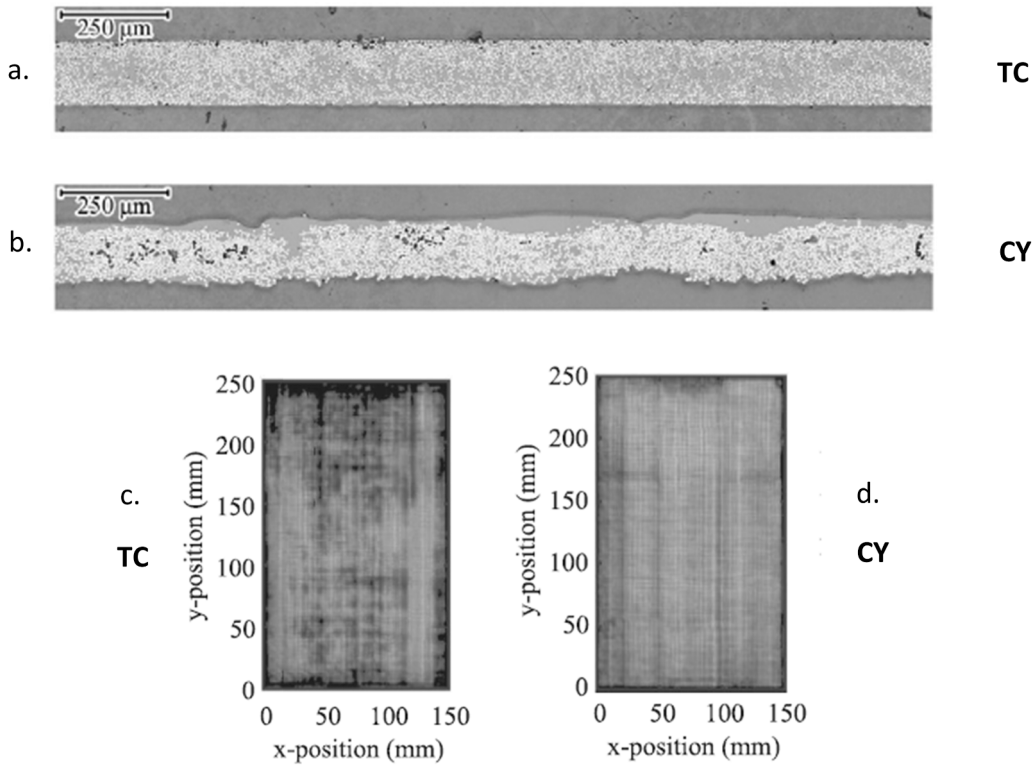

Fig. 13. Cross-sectional micrographs of the as-received a. TC prepreg and b. CY prepreg. Corresponding US C-scans after stamp forming (at 390 °C and 20 bar) of c. TC and d. CY tapes placed by AFP.
Reprinted from Slange et al. [123], ©2019 with permission from Elsevier.

before stamping.

To conclude, and despite some contradictory results in the literature, it is generally assumed that tapes with high roughness will lead to an increase in the time for intimate contact especially if fibers are present at the ply interface. On the other hand, tapes that are too smooth may prevent the volatiles from evacuating through interlaminar voids. A compromise consisting in a richer resin surface while maintaining a sufficient roughness to enable volatiles evacuation might facilitate the consolidation step. Another compromise shall also be reached in terms of initial void content within the tapes: sufficient to ease the removal of volatiles (see also section below), but which also can be lowered significantly during the consolidation step.

4.2. Optimization of the processing parameters

4.2.1. Tape preparation before consolidation

The diffusion of volatiles can affect the final void content of the composite, and in some cases even causes deconsolidation. Understanding the evacuation of volatiles during the consolidation step, especially during OOA, is then crucial.

The main volatiles are:

1. Water (moisture), absorbed in the polymer and in the tape.
2. Air, trapped during the tape manufacturing step and/or during the lay-up.
3. Organic volatiles from the polymer synthesis and tape preparation.

Absorbed water (around 0.3% of matrix at 50 °C and 50% relative humidity [129]) is meant to be evacuated during the consolidation cycle, when the temperature is above T_g. Since the diffusion coefficient of water in CF/PAEK is small (around 4–6.10^{-13} m^2/s at 60 °C for CF/PEEK [130,131]) some water vapor will remain in the composite. Slange et al. [45] observed that thermal expansion of dissolved moisture can be responsible for deconsolidation in CF/PEEK. As shown in Fig. 14, (i) the composite displays an initial content of dissolved moisture within the matrix. Then, (ii) when the temperature increases, the water molecules start to diffuse through the ply-thickness. The diffusion is accelerated when the temperature is above T_g because of the increase in chain mobility. As the temperature increases, the water exerts more and more pressure on the specimen. (iii) When the temperature reaches T_m, the water will increase the voids size because the matrix can no longer sustain the pressure induced by the water vapor, which leads to an increase in the specimen thickness. (iv) Voids start to merge and create

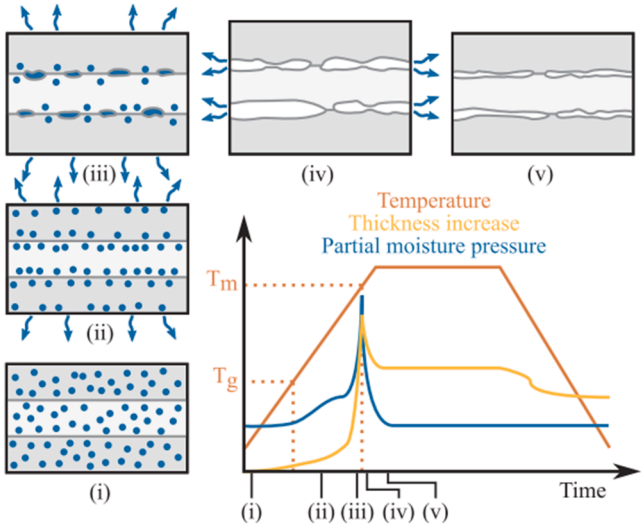

Fig. 14. Schematic representation of the deconsolidation phenomenon due to moisture expansion
Reprinted from Slange et al. [45], ©2018 with permission from Elsevier.

channels between the plies enabling the water to diffuse more easily. (v) The internal void pressure decreases and the thickness decreases again [45]. As also explained in [45], it is possible to reduce deconsolidation due to water by drying the specimen before the consolidation step. Drying CF/PEEK laminates at 250 °C for 3 h can prevent from such deconsolidation [45].

Air trapped in the composite has the same effect as moisture on the deconsolidation behavior of laminates [14,69,132]. Swamy et al. [69] detail the two phenomena responsible for the volatiles evacuation during consolidation: first the gazes diffuse through the composite and then are removed through evacuation channels. Hence, a denser laminate will lead to diffusion through the entire composite thickness, which can take a time higher than the consolidation one. For well pre-consolidated AFP laminates, drying before consolidation may then be a necessary step to avoid possible deconsolidation. The authors therefore insist on the beneficial role of gaps induced during AFP to enable "in-plane air evacuation" during the next processing step, but adding these interlayer gaps will affect consolidation, especially for short-time processes.

To evaluate the pre-consolidation quality of a laminate, Slange et al. [133,134] proposed to measure the thermal gradient between the surface (continuous lines in Fig. 15) and the middle of the sample (dash lines in Fig. 15). For example, this gradient is way more important for the USSW (UltraSonic Spot Welding) pre-consolidated laminates (more than 50 °C of difference between the surface and the middle of the laminate) than for those pre-consolidated by press or AFP, showing the weak inter-laminar bonds created during USSW compared to the two other methods.

4.2.2. *Optimization of the prepreg ATP lay-up process*

First, note that optimizing the ATP lay-up process is obviously much more critical for "in-situ" consolidation than for press, autoclave or even VBO consolidation.

The relevant parameters involved in ATP process have been reviewed by Khaled et al. [16]. Khan et al. [50] evaluated the degree of bonding of CF/PEEK laminates, manufactured through AFP with different processing parameters (heating cycle, layup velocity, and roller pressure), through Interlaminar Shear Strength (ILSS) measurements. This adapted 3-point bending test characterizes the resistance to interply shear.

High heating and cooling rates as well as short-term pressure make it challenging to obtain a well pre-consolidated laminate [55,62,135]. A good control on the temperature must be reached: low temperatures will lead to high viscosities that will prevent void content reduction and consolidation at the interfaces, and high temperatures may induce thermal degradation of the composite, as CF/PEEK tapes can reach temperatures above 500 °C [64,73,76,77,82]. The temperature at the nip point (see Fig. 4) then needs to be precisely monitored during the ATP process, which is complicated to achieve. For hot gas torch heating, only the temperature of the heat source can be monitored precisely, which will induce differences between the temperature of the tape being deposited and the one of the already stacked tapes [16,70]. For laser heating, due to the curvature of the tape and the roll (see Fig. 4), a thermal gradient takes place between the locally heated zone and the nip point, known as the shadowing effect [76] (see Fig. 4). It can also be mentioned that the width of the incoming tapes and/or the diameter of the heating source hampers the control of the temperature. One then needs to place adequately (both in terms of angle and distance) the heat source and impose a temperature sufficient to consolidate at the nip point without degrading the material [18].

The roller pressure is another ATP fundamental parameter. As stated in [50], increasing the roller pressure enhances voids reduction and leads to a larger contact area between the roller and the top layer for consolidation. It is proposed to use a large roller to dissipate enough energy from the plies such that, after the pass of the roller, the temperature of the top ply decreases rapidly below T_g, thus avoiding deconsolidation. However, applying a high pressure while using a large roller demands a high force delivered by the head, which might be challenging. This is all the more true that according to Çelik et al. [73], the relation between compaction pressure and compaction force is not linear because of the deformation of the roller. Schledjewski et al. [58] suggest the use of an adaptative roller, i.e. capable of moving in the plan of the stacked tapes while increasing the roller pressure, in order to provide a homogeneous pressure and correct the potential misalignment between the tool (see Fig. 4) and the roller. Even if an increase in the roller pressure supposes a better bonding strength at the ply interface, Qureshi et al. [59] did not evidence a correlation between ILSS and compaction pressure for CF/PEEK composites, maybe due to the fact that the pressure used was already sufficient to provide good intimate contact.

Heating rate, and even more, cooling rate will also influence the bonding quality of the laminate. In general the AFP cooling rate is very high (up to 300 °C/s [16]) leading to a nearly glassy matrix, even for rapid crystallization rates evidenced for PEKK [35] and PEEK [136]. Such rapid cooling rates can increase residual stresses within the plies [137], which can lead to delamination or matrix cracking in the next processing steps. Khaled et al. [16] then suggest that slowing the cooling can lead to an increase in the composite crystallinity [121] and hence a higher strength at the ply interface. The cooling rate can be lowered by increasing the tool temperature. However, one has to keep in mind that the remaining porosities may be another cause for poor mechanical

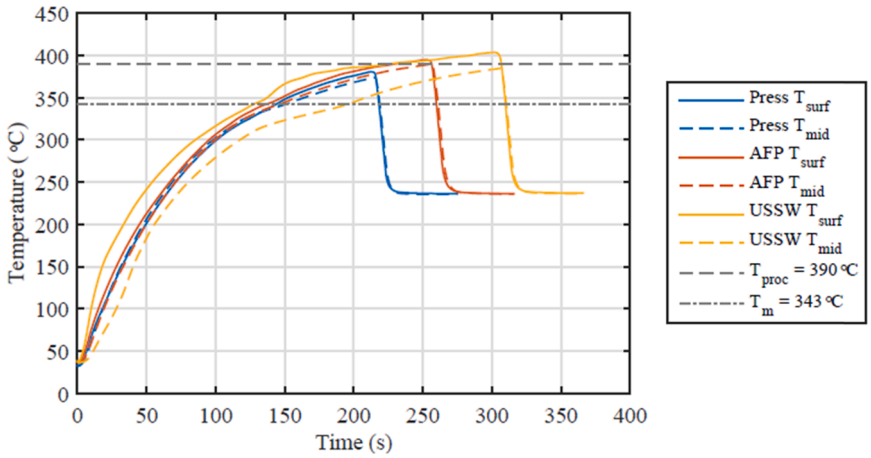

Fig. 15. Measured temperatures of the surface and the mid-plane of CF/PEEK laminates during stamp forming for different pre-consolidation methods. Reprinted from Slange [134], ©2019, University of Twente.

properties. Chen et al. [121] concluded that the ILSS and compression strength of CF/polyphenylene sulfide (PPS) composites depend much more on void content and porosity distribution and dispersion than on crystallinity.

Layup velocity (or deposing head velocity) is the speed of the plies' placement during AFP process. It can highly influence the pre-consolidation quality of the laminate by affecting the cooling rate. Khan et al. [50] explain that low velocities (3 m/min) leads to good bonding strengths because longer time exposures improve the polymer healing. Stokes-Griffin et al. [76] show that at lower placement rates, CF/PEEK composites exhibit better fiber-matrix adhesion but a more brittle behavior because of higher crystallinity achieved. In another study [77], the same authors evidenced that at high layup velocities, the specimen is under the consolidation zone for a time below the one required for crystallization. Hence, the polymer is in glassy state during the development of inter-laminar bonds, enabling the autohesion to occur below T_m on the next processing steps. Of course, a balance between layup velocity and productivity has to be reached.

The number of passes of the roller on the tapes for the AFP process is also playing a role on the final consolidation quality of the composite. Increasing the number of passes increases the intimate contact and lead to a lower inter-laminar void content (and thus a better pre-consolidated laminate) [16,72]. The effect of the number of passes on ILSS has not been clearly evidenced yet: Khan et al. [50] found for example that ILSS increases from 81 to 88 MPa after 3 repasses on CF/PEEK composites. However, in a study by Mantell et al. also on CF/PEEK [52], ILSS does not significantly increase with the number of passes despite an improvement of the degree of intimate contact. Similar results were also obtained by Chanteli et al. [70]. Repassing also affects the surface finish of the laminate. Chanteli et al. [70] measured a lower surface roughness (R_a) along the fibers on CF/PEEK composites with two passes (from 4.9 μm to 2 μm). Shadmehri et al. [63] describes an even greater decrease of R_a (from 40 μm to 6 μm and from 19 μm to 2.6 μm, respectively in the directions transverse and parallel to the fibers) for similar conditions and composites. Tierney et al. [122,138] also suggest to increase the number of passes as well as the layup velocity so that voids are more easily reduced and locked at temperatures just above T_g. [50] It shall also be mentioned that during AFP, the first incoming tapes are heated above T_m and then cooled several times as the subsequent plies are placed, enabling more time for intimate contact and healing than the last ones. Disparities in terms of consolidation level can then be observed within the composite thickness [18,138]. Hence, it is recommended to apply few repasses, at least on the last plies, to decrease the whole void content of the laminate [63,70,72]. These repasses may also have an effect on the crystallinity, which is still debated in the literature. While Comer et al. [55] mention an increase in crystallinity with increasing number of repasses, Chanteli et al. [70] do not observe any effect. Finally, Shadmehri et al. [63] showed a decrease from 30% to 24% in the degree of crystallinity after two repasses also on CF/PEEK.

To conclude, one should mention that too many passes may degrade thermally the matrix [50]. An optimized number of passes shall then be sought for and consider the composite thickness.

Note that several heat source parameters also need optimization to improve the final consolidation of the composite. They have been reviewed in detail by Khaled et al. [16] and will not be discussed further on in this review.

4.2.3. Optimization of the consolidation process

Consolidation of the laminate is the final step to obtain a void-free composite. It is mandatory to optimize the processing parameters involved in this step, which are mainly, pressure, temperature and time. Similar to the prepreg lay-up, the chosen temperature shall enable sufficient flow without degrading the matrix. High pressure will favor the development of intimate contact hence the bonding strength between the plies. The time for consolidation shall be high enough to promote sufficient healing and void reduction as well as a proper evacuation of volatiles (air, water, …) [139]. Slange et al. [123,133] showed that CF/PEEK laminates obtained through AFP followed by stamp forming have lower flexural strengths than those obtained by press or autoclave despite the higher pressure applied, because the fast consolidation through stamp forming does not enable the matrix to crystallize as well as with longer processes.

The optimized parameters for autoclave or press consolidation are now relatively well-known [140] but since an interest for out-of-autoclave processes is emerging, the following paragraph will deal specifically with VBO. Saffar et al. [57,68] developed two VBO processes for CF/PEKK composites, one in an oven and one using a heating plate. For the heating plate configuration, a heterogeneous distribution of the heat through the sample thickness has been measured, as well as an important variation of the final composite thickness due to a difference of pressure homogeneity along the surface of the laminate. Typically, the laminate is thinner (i.e. better consolidated) near the pump evacuation hole than at the opposite side. Concerning the oven system, the temperature applied on the laminate is relatively well distributed [57,68]. They also concluded that a pressure at least equal to 800 mbar is necessary to prevent the laminate from deconsolidation and get a dense component with ILSS values close to those obtained by press. This pressure must be maintained at the required value during all the consolidation cycle, which is possible by maintaining a high level of vacuum under the bag [125]. A similar trend has been observed by Levy et al. [141] for complex molds in OOA systems under oven: a deviation of the laminate thickness happens at the corner because of a heterogeneous pressure distribution linked to the geometry of the mold. This leads to an increase of the porosity as well as areas rich either in fibers or in resin at the corner. Centea et al. [125] also headline the difficulty of maintaining a homogeneous pressure when the size of the laminate increases.

As mentioned before, AFP "in-situ" consolidation is the most promising technique to achieve high-productivity, and thus has been the subject of recent research [15,18,58,59]. The optimization of the heat source parameters, roller pressure, temperature, layup velocity developed in the previous section, are obviously needed as well to improve "in-situ" consolidation.

One of the main issues is the very short time dedicated to the healing process. Indeed, a high pressure and a smooth tape will decrease the intimate contact time but, as mentioned before, the time to achieve complete healing is constant for a given resin and higher than the one spent above T_m during AFP under typical conditions (less than 1 s [77]). A higher number of passes may lead to an improvement of healing but will increase the processing time.

A second consequence of this short processing time is the fact that it will lead to low degrees of crystallinity, hence lower mechanical properties for the composite. To solve this, Schiel et al. [61] propose to anneal afterwards the obtained laminate at a temperature above T_g. Alternatively, increasing the tool temperature leads to lower cooling rates and higher degree of crystallinity as well.

Another issue for "in-situ" consolidation is fiber stress-release. During the pre-impregnation step, the elastic energy of the fiber network is stored in the composite under the form of residual stresses because of a difference of thermal expansion coefficients between fibers and matrix [18,142]. The release of these stresses is called de-compaction of fiber reinforcement [49]. Slange et al. [45] claim that the time above T_m during AFP is too short to let fibers release their accumulated stress, which may be an issue for "in-situ" consolidation and subsequent welding of parts.

Degradation during "in-situ" consolidation has been reviewed by Martin et al. [18]. The temperature at the tape level can reach values above 500 °C, even though for very short times [143]. Bayerl et al. [144] showed that CF/PEEK composites start to degrade after only 100 ms of heat exposure for laser powers above 100 W. Hence, increasing the number of passes or decreasing the layup velocity may lead to degradation.

Finally, defects are induced when steering tapes during AFP process, due to the roller imperfections. For straight steered tapes, gaps and overlaps are mainly generated [86,120,145,146], preventing from "in-situ" consolidation. Gaps create a local reduction in the laminate thickness whereas overlaps locally increase it. These defects lead to a decrease in the tensile strength [147] and in the compressive strength [147,148]. For L-shaped laminates, overlaps may have a positive effect as the local excess material counteracts the thickness reduction at the angles [149]. For curved steered tapes, the radius of curvature plays an important role on the final properties of the laminate. Recent studies on CF/PEEK composites show that lowering the steering radius increases defects such as fiber folding / wrinkling [150] as well as the thickness of the laminate at the expense of its width [150,151]. Rajasekaran et al. [151] also showed that decreasing the steering radius below 400 mm decreases the lap shear strength (LSS) from 21 MPa to 15 MPa, far below the LSS of autoclave processed samples (49 MPa). An additional processing step, as suggested by Kermani et al. [120] is then often necessary to fill these gaps [86] and obtain a well-consolidated composite.

To conclude, if "in-situ" consolidation directly during AFP seems to be the future solution in terms of productivity, the seemingly contradictory issues discussed above limit its current use and the need for OOA consolidation.

As a final note, additive manufacturing is also currently developed for CF/PAEK composites, especially to achieve complex geometries, and has been recently reviewed by Struzziero et al. [152].

5. Conclusion

Consolidation of CF/PAEK composites, especially with out-of-autoclave and "in-situ" processes is still under optimization to answer totally the current industrial needs, especially in the aerospace sector. This review gives an insight of the physical and physicochemical phenomena involved during consolidation, with a special focus on the rheology of CFRTP. The flowing under compression of such multiphase materials containing multiple layers, continuous fibers and a highly-viscous matrix is extremely complex. Different mechanisms, from the micro to the macro-scale, are coupled or dominate at different time-scales. In particular, a proper experimental characterization and/or modeling of the viscosity of such composites is still needed, and should consider fiber locking, flow anisotropy and possible slip at the interface.

To increase the quality of such composites, several suggestions can be explored in future research, including tapes with low roughness, a good fiber/matrix distribution, a low initial void content and resin-rich regions at the surface. A well-defined drying process will also help to avoid deconsolidation due to thermal expansion of dissolved moisture and other volatiles during the consolidation cycle. Optimization of several lay-up or consolidation parameters is still lacking and probably requires a more systematic design of experiments which could beneficiate from efficient simulation tools [153].

Solving the paradoxes of "in-situ" consolidation, where short consolidation times must lead to high-quality composites, will certainly be the objective of many collaborations between industrial and academic partners to come.

CRediT authorship contribution statement

Raphaël Arquier: Methodology, Investigation, Writing – original draft, Visualization. **Ilias Iliopoulos:** Writing – review and editing, Supervision, Project administration, Funding acquisition. **Gilles Régnier:** Formal Analysis, Writing – review and editing, Supervision. **Guillaume Miquelard-Garnier:** Conceptualization, Writing – original draft, Supervision.

Declaration of Competing Interest

The authors declare that they have no known competing financial interests or personal relationships that could have appeared to influence the work reported in this paper.

Data Availability

This is a review article. Data presented do not come from the authors. The availability of the data may differ for each of the data presented in the review.

Acknowledgements

This work was conducted under the framework of HAICoPAS, a PSPC project (projet de recherche et développement structurant pour la compétitivité) and of the Industrial Chair Arkema (Arkema/ CNTS-ENSAM-Cnam). BPI France is acknowledged for funding the PhD work of R. Arquier (project number: PSPC.AAP-7.0_HAICoPAS). The authors finally thank Arkema, Hexcel, and more specifically Lucien Fiore, Stéphanie Lambour, Nicolas Cadorin, Mayeul Ducrot, Michel Glotin, Henri-Alexandre Cayzac, Jérôme Pascal, Yves Deyrail and Sylvie Tencé-Girault for fruitful discussions. Bruno Fayolle and Gwladys Lesimple, from the PIMM laboratory, are also acknowledged.

References

[1] H.Y. Zhang, L.L. Yuan, W.J. Hong, S.Y. Yang, Improved melt processabilities of thermosetting polyimide matrix resins for high temperature carbon fiber composite applications, Polymers (2022) 14, https://doi.org/10.3390/polym14050965.

[2] B.A. Bulgakov, A.V. Sulimov, A.V. Babkin, D.V. Afanasiev, A.V. Solopchenko, E. S. Afanaseva, et al., Flame-retardant carbon fiber reinforced phthalonitrile composite for high-temperature applications obtained by resin transfer molding, Mendeleev Commun. 27 (2017) 257–259, https://doi.org/10.1016/j.mencom.2017.05.013.

[3] L.F.M. Da Silva, R.D. Adams, M. Gibbs, Manufacture of adhesive joints and bulk specimens with high-temperature adhesives, Int J. Adhes. Adhes. 24 (2004) 69–83, https://doi.org/10.1016/S0143-7496(03)00101-5.

[4] M. Thunga, K. Larson, W. Lio, T. Weerasekera, M. Akinc, M.R. Kessler, Low viscosity cyanate ester resin for the injection repair of hole-edge delaminations in bismaleimide/carbon fiber composites, Compos Part A Appl. Sci. Manuf. 52 (2013) 31–37, https://doi.org/10.1016/j.compositesa.2013.05.001.

[5] H.K. Kung, Effects of surface roughness on high-temperature oxidation of carbon-fiber-reinforced polyimide composites, J. Compos Mater. 39 (2005) 1677–1687, https://doi.org/10.1177/0021998305051801.

[6] H.M. El-Dessouky, C.A. Lawrence, Ultra-lightweight carbon fibre/thermoplastic composite material using spread tow technology, Compos Part B Eng. 50 (2013) 91–97, https://doi.org/10.1016/j.compositesb.2013.01.026.

[7] Clyne T.W., Hull D. An Introduction to Composite Materials. Second Edi. In: Cambridge Solid State Science Series; 2019.

[8] U.K. Vaidya, K.K. Chawla, Processing of fibre reinforced thermoplastic composites, Int Mater. Rev. 53 (2008) 185–218, https://doi.org/10.1179/174328008X325223.

[9] T. Choupin, B. Fayolle, G. Régnier, C. Paris, J. Cinquin, B. Brulé, Isothermal crystallization kinetic modeling of poly(etherketoneketone) (PEKK) copolymer, Polym. (Guildf.) 111 (2017) 73–82, https://doi.org/10.1016/j.polymer.2017.01.033.

[10] R. McCool, A. Murphy, R. Wilson, Z. Jiang, M. Price, J. Butterfield, et al., Thermoforming carbon fibre-reinforced thermoplastic composites, Proc. Inst. Mech. Eng. Part L J. Mater. Des. Appl. 226 (2012) 91–102, https://doi.org/10.1177/1464420712437318.

[11] T. Choupin, B. Fayolle, G. Régnier, C. Paris, J. Cinquin, A more reliable DSC-based methodology to study crystallization kinetics: application to poly (ether ketone ketone) (PEKK) copolymers, Polym. (Guildf.) 155 (2019) 109–115, https://doi.org/10.1016/j.polymer.2018.08.060.

[12] D. Veazey, T. Hsu, E.D. Gomez, Next generation high-performance carbon fiber thermoplastic composites based on polyaryletherketones, J. Appl. Polym. Sci. 134 (2017) 19–21, https://doi.org/10.1002/app.44441.

[13] S. Van Hoa, M. Duc Hoang, J. Simpson, Manufacturing procedure to make flat thermoplastic composite laminates by automated fibre placement and their mechanical properties, J. Thermoplast. Compos Mater. 30 (2017) 1693–1712, https://doi.org/10.1177/0892705716662516.

[14] D. Zhang, Void consolidation of thermoplastic composites via non-autoclave processing, University of Delaware, Newark, USA, 2017. PhD Thesis.

[15] Di Boon Y, S.C. Joshi, S.K. Bhudolia, Review: Filament winding and automated fiber placement with in situ consolidation for fiber reinforced thermoplastic polymer composites, Polymers 13 (2021), https://doi.org/10.3390/polym13121951.

[16] Y. Khaled, H. Mehdi, Processing of thermoplastic matrix composites through automated fiber placement and tape laying methods: a review, J. Thermoplast. Compos Mater. (2017) 1–50, https://doi.org/10.1177/0892705717738305.

[17] H. Pérez-Martín, P. Mackenzie, A. Baidak, C.M. Ó Brádaigh, D. Ray, Crystallinity studies of PEKK and carbon fibre/PEKK composites: a review, Compos Part B Eng. (2021) 223, https://doi.org/10.1016/j.compositesb.2021.109127.

[18] I. Martin, D. Saenz Del Castillo, A. Fernandez, A. Güemes, Advanced thermoplastic composite manufacturing by in-situ consolidation: a review, J. Compos Sci. 4 (2020) 1–36, https://doi.org/10.3390/jcs4040149.

[19] G. Struzziero, J.J. Teuwen, A. Skordos, Numerical optimisation of thermoset composites manufacturing process: a review, Compos Part A Appl. Sci. Manuf. (2019) 124, https://doi.org/10.1016/j.compositesa.2019.105499.

[20] J. Wang, X. Ge, Y. Liu, Z. Qi, L. Li, S. Sun, et al., A review on theoretical modelling for shearing viscosities of continuous fibre-reinforced polymer composites, Rheol. Acta 58 (2019) 321–331, https://doi.org/10.1007/s00397-019-01151-1.

[21] A.M. Díez-Pascual, M. Naffakh, C. Marco, G. Ellis, M.A. Gómez-Fatou, High-performance nanocomposites based on polyetherketones, Prog. Mater. Sci. 57 (2012) 1106–1190, https://doi.org/10.1016/j.pmatsci.2012.03.003.

[22] T. Choupin, L. Debertrand, B. Fayolle, G. Régnier, C. Paris, J. Cinquin, et al., Influence of thermal history on the mechanical properties of poly(ether ketone ketone) copolymers, Polym. Cryst. 2 (2019) 1–8, https://doi.org/10.1002/pcr2.10086.

[23] Arkema. Kepstan PEKK ®. Tech Data Sheet 2018.

[24] L. Quiroga Cortés, N. Caussé, E. Dantras, A. Lonjon, C. Lacabanne, Morphology and dynamical mechanical properties of poly ether ketone ketone (PEKK) with meta phenyl links, J. Appl. Polym. Sci. 133 (2016) 1–10, https://doi.org/10.1002/app.43396.

[25] M.F. Talbott, G.S. Springer, L.A. Berglund, The effects of crystallinity on the mechanical properties of PEEK polymer and graphite fiber reinforced PEEK, J. Compos Mater. 21 (1987) 1056–1081, https://doi.org/10.1177/002199838702101104.

[26] M.L. Minus, S. Kumar, The processing, properties, and structure of carbon fibers, Jom 57 (2005) 52–58, https://doi.org/10.1007/s11837-005-0217-8.

[27] K. Wang, S. Pei, Y. Li, J. Li, D. Zeng, X. Su, et al., In-situ 3D fracture propagation of short carbon fiber reinforced polymer composites, Compos Sci. Technol. 182 (2019), 107788, https://doi.org/10.1016/j.compscitech.2019.107788.

[28] Q. Zhang, J. Zhang, L. Wu, Impact and energy absorption of long fiber-reinforced thermoplastic based on two-phase modeling and experiments, Int J. Impact Eng. 122 (2018) 374–383, https://doi.org/10.1016/j.ijimpeng.2018.09.003.

[29] H. Rolland, N. Saintier, G. Robert, Damage mechanisms in short glass fibre reinforced thermoplastic during in situ microtomography tensile tests, Compos Part B Eng. 90 (2016) 365–377, https://doi.org/10.1016/j.compositesb.2015.12.021.

[30] D. Deborah, L. Chung. Carbon Fiber Composites, first ed., Elsevier. Butterworth-Heinemann, 1994.

[31] J. Vinodhini, K. Sudheendra, Influence of argon plasma treatment on carbon fibre reinforced high performance thermoplastic composite, High. Perform. Polym. 33 (2021) 285–294, https://doi.org/10.1177/0954008320957062.

[32] B. Wu, G. Zheng, Synergistic modification of carbon fiber by electrochemical oxidation and sizing treatment and its effect on the mechanical properties of carbon fiber reinforced composites, J. Appl. Polym. Sci. 48028 (2019) 1–10, https://doi.org/10.1002/app.48028.

[33] I. Giraud, S. Franceschi-Messant, E. Perez, C. Lacabanne, E. Dantras, Preparation of aqueous dispersion of thermoplastic sizing agent for carbon fiber by emulsion/solvent evaporation, Appl. Surf. Sci. 266 (2013) 94–99, https://doi.org/10.1016/j.apsusc.2012.11.098.

[34] B.S. Hsiao, I.Y. Chang, B.B. Sauert, Isothermal crystallization kinetics of poly (ether ketone ketone) and its carbon-fibre-reinforced composites, Polym. (Guildf.) (1991) 32, https://doi.org/10.1016/0032-3861(91)90111-U.

[35] T. Choupin, Mechanical performances of PEKK thermoplastic composites linked to their processing parameters. PhD Thesis, Ecole Nationale des Supérieure des Arts et Métiers,, Paris, 2017.

[36] K.K.C. Ho, S. Shamsuddin, S. Riaz, S. Lamorinere, M.Q. Tran, A. Javaid, et al., Wet impregnation as route to unidirectional carbon fibre reinforced thermoplastic composites manufacturing, Plast. Rubber Compos 40 (2011) 100–107, https://doi.org/10.1179/174328911X12988622801098.

[37] M. Connor. Consolidation Mechanisms and Interfacial Phenomena in Thermoplastic Powder Impregnated Composites, Ecole Polytechnique Federale de Lausanne, 1995. PhD Thesis.

[38] K. Kawabe, New Spreading technology for carbon fiber tow and its application to composite materials, Fiber 64 (8) (2008) 262–267, https://doi.org/10.2115/fiber.64.P_262.

[39] K. Kawabe, Z.-I.M. Matsuo T, Next technology for opening various reinforcing fiber tows, J. Soc. Mater. Sci. Jpn. 47 (7) (1998) 727–734, https://doi.org/10.2472/jsms.47.727.

[40] J. Quintana Casanovas, J. Costa, J.A. Mayugo, A. Galan Llongueras, Fabrication of hybrid thin ply tapes, IOP Conf. Ser. Mater. Sci. Eng. (2018) 406, https://doi.org/10.1088/1757-899X/406/1/012067.

[41] A. Arteiro, C. Furtado, G. Catalanotti, P. Linde, P.P. Camanho, Thin-ply polymer composite materials: a review, Compos Part A Appl. Sci. Manuf. (2020) 132, https://doi.org/10.1016/j.compositesa.2020.105777.

[42] D.H.A. Lukaszewicz, C. Ward, K.D. Potter, The engineering aspects of automated prepreg layup: history, present and future, Compos Part B 43 (2012) 997–1009, https://doi.org/10.1016/j.compositesb.2011.12.003.

[43] K. Yassin, M. Hojjati, Processing of thermoplastic matrix composites through automated fiber placement and tape laying methods: a review, J. Thermoplast. Compos Mater. 31 (2018) 1676–1725, https://doi.org/10.1177/0892705717738305.

[44] R.H. Rizzolo, D.F. Walczyk, Ultrasonic consolidation of thermoplastic composite prepreg for automated fiber placement, J. Thermoplast. Compos Mater. (2015) 1–18, https://doi.org/10.1177/0892705714565705.

[45] T.K. Slange, L.L. Warnet, W.J.B. Grouve, R. Akkerman, Deconsolidation of C/PEEK blanks: on the role of prepreg, blank manufacturing method and conditioning, Compos Part A Appl. Sci. Manuf. 113 (2018) 189–199, https://doi.org/10.1016/j.compositesa.2018.06.034.

[46] N. Selles, N. Saintier, L. Laiarinandrasana, Voiding mechanisms in semi-crystalline polyamide 6 during creep tests assessed by damage based constitutive relationships and finite elements calculations, Int J. Plast. 86 (2016) 112–127, https://doi.org/10.1016/j.ijplas.2016.08.004.

[47] L. Laiarinandrasana, T.F. Morgeneyer, H. Proudhon, F. N'Guyen, E. Maire, Effect of multiaxial stress state on morphology and spatial distribution of voids in deformed semicrystalline polymer assessed by X-ray tomography, Macromolecules 45 (2012) 4658–4668, https://doi.org/10.1021/ma3005247.

[48] B. Landry, P. Hubert, Experimental study of defect formation during processing of randomly-oriented strand carbon/PEEK composites, Compos Part A Appl. Sci. Manuf. 77 (2015) 301–309, https://doi.org/10.1016/j.compositesa.2015.05.020.

[49] L. Ye, M. Lu, Y.-W. Mai, Thermal de-consolidation of thermoplastic matrix composites—I. Growth of voids, Compos Sci. Technol. 62 (2002) 2121–2130, https://doi.org/10.1016/S0266-3538(02)00144-6.

[50] M.A. Khan, P. Mitschang, R. Schledjewski, Identification of some optimal parameters to achieve higher laminate quality through tape placement process, Adv. Polym. Technol. 29 (2010) 98–111, https://doi.org/10.1002/adv.20177.

[51] J.E. Manson, T.L. Schneider, J.C. Seferis, Press-forming of continuous-fiber-reinforced thermoplastic composites, Polym. Compos (1990) 11, https://doi.org/10.1002/pc.750110207.

[52] S.C. Mantell, W. Qiuling, G.S. Springer, Processing thermoplastic composites in a press and by tape laying—experimental results, J. Compos Mater. 26 (1992) 2378–2401, https://doi.org/10.1177/002199839202601603.

[53] A. Lystrap, T.L. Andersen, Autoclave consolidation of fibre composites with a high temperature thermoplastic matrix, J. Mater. Process Technol. 300 (1998) 80–85, https://doi.org/10.1016/s0924-0136(97)00398-1.

[54] J.A.E. Manson, J.C. Seferis, Autoclave processing of PEEK/Carbon fiber composites, J. Thermoplast. Compos Mater. 2 (1989) 34–49, https://doi.org/10.1177/089270578900200103.

[55] A.J. Comer, D. Ray, W.O. Obande, D. Jones, J. Lyons, I. Rosca, et al., Mechanical characterisation of carbon fibre-PEEK manufactured by laser-assisted automated-tape-placement and autoclave, Compos Part A Appl. Sci. Manuf. 69 (2015) 10–20, https://doi.org/10.1016/j.compositesa.2014.10.003.

[56] F. Saffar, C. Sonnenfeld, P. Beauchêne, C.H. Park, Influence of Process Parameters on the Quality of Carbon/PEKK Laminates Manufactured by Out-of-autoclave Consolidation, ECCM 2018 - 18th Eur. Conf. Compos. Mater., Athens, Greece, 2018, pp. 24–28.

[57] F. Saffar, Etude de la consolidation interpli de stratifiés thermoplastiques PEKK / fibres de carbone en conditions de basse pression. PhD Thesis, Ecole Nationale Supérieure Mines-Télécom Lille Douai, 2020.

[58] R. Schledjewski, Thermoplastic tape placement process - In situ consolidation is reachable, Plast. Rubber Compos 38 (2009) 379–386, https://doi.org/10.1179/146580109X12540995045804.

[59] Z. Qureshi, T. Swait, R. Scaife, H.M. El-Dessouky, In situ consolidation of thermoplastic prepreg tape using automated tape placement technology: Potential and possibilities, Compos Part B Eng. 66 (2014) 255–267, https://doi.org/10.1016/j.compositesb.2014.05.025.

[60] V. Hoang, B. Kwon, J. Sung, H. Choe, S. Oh, S. Lee, et al., Postprocessing mechanical properties of carbon fiber-reinforced thermoplastic composites, J. Thermoplast. Compos Mater. (2020) 1–16, https://doi.org/10.1177/0892705720945376.

[61] I. Schiel, L. Raps, A.R. Chadwick, I. Schmidt, M. Simone, S. Nowotny, An investigation of in-situ AFP process parameters using CF/LM-PAEK, Adv. Manuf. Polym. Compos Sci. 6 (2020) 191–197, https://doi.org/10.1080/20550340.2020.1826772.

[62] D. Ray, A.J. Comer, J. Lyons, W. Obande, D. Jones, R.M.O. Higgins, et al., Fracture toughness of carbon fiber/polyether ether ketone composites manufactured by autoclave and laser-assisted automated tape placement, J. Appl. Polym. Sci. 132 (2015) 1–10, https://doi.org/10.1002/app.41643.

[63] F. Shadmehri, S.V. Hoa, J. Fortin-Simpson, H. Ghayoor, Effect of in situ treatment on the quality of flat thermoplastic composite plates made by automated fiber placement (AFP, Adv. Manuf. Polym. Compos Sci. 4 (2018) 41–47, https://doi.org/10.1080/20550340.2018.1444535.

[64] J. Avenet, A. Levy, J. Bailleul, S. Le Corre, J. Delmas, Adhesion of high performance thermoplastic composites: development of a bench and procedure for kinetics identification, Compos - Part A Appl. Sci. Manuf. (2020) 138, https://doi.org/10.1016/j.compositesa.2020.106054.

[65] K.B. Mahat, I. Alarifi, A. Alharbi, R. Asmatulu, Effects of UV light on mechanical properties of carbon fiber reinforced PPS thermoplastic composites, Macromol. Symp. 365 (2016) 157–168, https://doi.org/10.1002/masy.201650015.

[66] D. Saenz-Castillo, M.I. Martín, V. García-Martínez, A. Ramesh, M. Battley, A. Güemes, A comparison of mechanical properties and X-ray tomography analysis of different out-of-autoclave manufactured thermoplastic composites, J. Reinf. Plast. Compos 39 (2020) 703–720, https://doi.org/10.1177/0731684420924081.

[67] D. Zhang, D. Heider, J.W. Gillespie, Void reduction of high-performance thermoplastic composites via oven vacuum bag processing, J. Compos Mater. 51 (2017) 4219–4230, https://doi.org/10.1177/0021998317700700.

[68] F. Saffar, C. Sonnenfeld, P. Beauchêne, C.H. Park, In-situ monitoring of the out-of-autoclave consolidation of carbon / poly-ether-ketone-ketone prepreg laminate, Front. Mater. 7 (2020) 1–12, https://doi.org/10.3389/fmats.2020.00195.

[69] J.N. Swamy, S. Wijskamp, W.J.B. Grouve, R. Akkerman, Out of autoclave consolidation of fiber placed thermoplastic, Compos. Struct. (2020) 13–15, https://doi.org/10.13140/2.1.2632.5289.

[70] A. Chanteli, A. Kumar, D. Peeters, R.M.O. Higgins, P.M. Weaver, Influence of repass treatment on carbon fibre-reinforced PEEK composites manufactured using laser-assisted automatic tape placement, Compos Struct. 248 (2021), 112539, https://doi.org/10.1016/j.compstruct.2020.112539.

[71] S. Risteska, A.T. Petkoska, S. Samak, M. Drienovsky, Annealing effects on the crystallinity of carbon fiber-reinforced polyetheretherketone and polyohenylene laminate composites manufactured by laser automatic tape placement 26 (2020) 308–316, https://doi.org/10.5755/j01.ms.26.3.21489.

[72] M.A. Khan, P. Mitschang, V. Gmbh, E. Geb, Tracing the void content development and identification of its effecting parameters during, Polym. Polym. Compos 18 (2010) 1–15, https://doi.org/10.1177/096739111001800101.

[73] O. Çelik, J.J.E. Teuwen, Effects of Process Parameters on Intimate Contact Development in Laser Assisted Fiber Placement, Proc. 4th Autom. Compos. Manuf., Montreal, Canada, 2019.

[74] F. Yang, R. Pitchumani, Healing of thermoplastic polymers at an interface under nonisothermal conditions, Macromolecules 35 (2002) 3213–3224, https://doi.org/10.1021/ma010858o.

[75] C. Ageorges, L. Ye, M. Hou, Advances in fusion bonding techniques for joining thermoplastic matrix composites: A review, Compos - Part A Appl. Sci. Manuf. 32 (2001) 839–857, https://doi.org/10.1016/S1359-835X(00)00166-4.

[76] C.M. Stokes-Griffin, P. Compston, The effect of processing temperature and placement rate on the short beam strength of carbon fibre–PEEK manufactured using a laser tape placement process, Compos Part A Appl. Sci. Manuf. 78 (2015) 274–283, https://doi.org/10.1016/j.compositesa.2015.08.008.

[77] C.M. Stokes-Griffin, P. Compston, Investigation of sub-melt temperature bonding of carbon-fibre/PEEK in an automated laser tape placement process, Compos Part A Appl. Sci. Manuf. 84 (2016) 17–25, https://doi.org/10.1016/j.compositesa.2015.12.019.

[78] C. Ageorges, L. Ye, Y.W. Mai, M. Hou, Characteristics of resistance welding of lap shear coupons. . Part II. Consolidation, Compos Part A Appl. Sci. Manuf. 29 (1998) 911–919, https://doi.org/10.1016/S1359-835X(98)00023-2.

[79] F. Yang, R. Pitchumani, A fractal Cantor set based description of interlaminar contact evolution during thermoplastic composites processing, J. Mater. Sci. 36 (2001) 4661–4671, https://doi.org/10.1023/A:1017950215945.

[80] C.A. Butler, R.L. Mccullough, R. Pitchumani, J.W. Gillespie, An analysis of mechanisms governing fusion bonding of thermoplastic composites, J. Thermoplast. Compos Mater. 11 (1998) 338–363, https://doi.org/10.1177/089270579801100404.

[81] O. Çelik, D. Peeters, C. Dransfeld, J. Teuwen, Intimate contact development during laser assisted fiber placement: microstructure and effect of process parameters, Compos Part A Appl. Sci. Manuf. 134 (2020), 105888, https://doi.org/10.1016/j.compositesa.2020.105888.

[82] A. Levy, S. Le Corre, I. Fernandez Villegas, Modeling of the heating phenomena in ultrasonic welding of thermoplastic composites with flat energy directors, J. Mater. Process Technol. 214 (2014) 1361–1371, https://doi.org/10.1016/j.jmatprotec.2014.02.009.

[83] J. Thomasset, P.J. Carreau, B. Sanschagrin, G. Ausias, Rheological properties of long glass fiber filled polypropylene, J. Nonnewton Fluid Mech. 125 (2005) 25–34, https://doi.org/10.1016/j.jnnfm.2004.09.004.

[84] S.G. Advani, T.S. Creasy, Rheology of long discontinuous fiber thermoplastic composites, Rheol. Ser. 8 (1999) 843–892, https://doi.org/10.1016/S0169-3107(99)80010-0.

[85] S.G. Advani, T.S. Creasy, S.F. Shuler, Chapter 8 Rheology of long fiber-reinforced composites in sheetforming, in: D. Bhattacharyya (Ed.), Compos. Sheet Form, vol. 11, Composite Materials Series, Elsiever, 1997, pp. 323–369, https://doi.org/10.1016/S0927-0108(97)80010-0.

[86] P. Simacek, N.N. Kermani, V. Gargitter, S.G. Advani, Role of resin percolation in gap filling mechanisms during the thin ply thermosetting automated tape placement process, Compos Part A 152 (2022), 106677, https://doi.org/10.1016/j.compositesa.2021.106677.

[87] S.G. Advani, E.M. Sozer, L. Mishnaevsky Jr., Process Modeling in Composites Manufacturing, Second ed., vol. 56, CRC Press, 2003.

[88] F.N. Cogswell, The processing science of thermoplastic structural composites, Int Polym. Process 1 (1987) 157–165, https://doi.org/10.3139/217.870157.

[89] P.V. Kaprielian, J.M. O'Neill, Shearing flow of highly anisotropic laminated composites, Composites 20 (1989) 43–47, https://doi.org/10.1016/0010-4361(89)90681-2.

[90] S.P. Haanappel, R. Akkerman, Shear characterisation of uni-directional fibre reinforced thermoplastic melts by means of torsion, Compos Part A Appl. Sci. Manuf. 56 (2014) 8–26, https://doi.org/10.1016/j.compositesa.2013.09.007.

[91] A. Deignan, W.F. Stanley, M.A. McCarthy, Insights into wide variations in carbon fibre/polyetheretherketone rheology data under automated tape placement processing conditions, J. Compos Mater. 52 (2018) 2213–2228, https://doi.org/10.1177/0021998317740733.

[92] V. Kishore, C. Ajinjeru, A.A. Hassen, J. Lindahl, V. Kunc, C. Duty, Rheological behavior of neat and carbon fiber-reinforced poly(ether ketone ketone) for extrusion deposition additive manufacturing, Polym. Eng. Sci. 60 (2020) 1066–1075, https://doi.org/10.1002/pen.25362.

[93] J.A. Goshawk, V.P. Navez, R.S. Jones, Squeezing flow of continuous fibre-reinforced composites, J. Nonnewton Fluid Mech. 73 (1997) 327–342, https://doi.org/10.1016/S0377-0257(97)00049-9.

[94] W.F. Stanley, P.J. Mallon, Intraply shear characterisation of a fibre reinforced thermoplastic composite, Compos Part A Appl. Sci. Manuf. 37 (2006) 939–948, https://doi.org/10.1016/j.compositesa.2005.03.017.

[95] D.J. Groves, A characterization of shear flow in continuous fibre thermoplastic laminates, Composites 20 (1989) 28–32, https://doi.org/10.1016/0010-4361(89)90678-2.

[96] T.G. Rogers, Rheological characterization of anisotropic materials, Composites 20 (1989) 21–27, https://doi.org/10.1016/0010-4361(89)90677-0.

[97] D.J. Groves, D.M. Stocks, Rheology of thermoplastic-carbon fibre composite in the elastic and viscoelastic states, Compos Manuf. 2 (1991) 179–184, https://doi.org/10.1016/0956-7143(91)90137-6.

[98] S.P. Haanappel, Forming of UD fibre reinforced thermoplastics, University of Twente, Enschede, the Netherlands, 2013. PhD Thesis.

[99] D.J. Groves, A.M. Bellamy, D.M. Stocks, Anisotropic rheology of continuous fibre thermoplastic composites, Composites 23 (1992) 75–80, https://doi.org/10.1016/0010-4361(92)90107-6.

[100] A. Deignan, Figiel, M.A. McCarthy, Insights into complex rheological behaviour of carbon fibre/PEEK from a novel numerical methodology incorporating fibre friction and melt viscosity, Compos Struct. 189 (2018) 614–626, https://doi.org/10.1016/j.compstruct.2018.01.084.

[101] P.C.F. Møller, S. Rodts, M.A.J. Michels, D. Bonn, Shear banding and yield stress in soft glassy materials, Phys. Rev. E Stat. Nonlinear, Soft Matter Phys. 77 (2008) 1–5, https://doi.org/10.1103/PhysRevE.77.041507.

[102] S. Shuler, S. Advani, Transverse squeeze flow of concentrated aligned fibers in viscous fluids, J. Non Newton Fluid Mech. 65 (1996) 47–74, https://doi.org/10.1016/0377-0257(96)01440-1.

[103] K.B. Thattaiparthasarthy, S. Pillay, U.K. Vaidya, Rheological characterization of long fiber thermoplastics - effect of temperature, fiber length and weight fraction, Compos Part A Appl. Sci. Manuf. 40 (2009) 1515–1523, https://doi.org/10.1016/j.compositesa.2009.06.009.

[104] J. Stefan, Versuche über die scheinbare Adhäsion, Ann. Phys. Chem. 230 (1875) 316–318, https://doi.org/10.1002/andp.18752300213.

[105] P. Leider, R. Bird, Squeezing flow between parallel disks. I. Theoretical Analysis, Ind. Eng. Chem. 13 (1974) 336–341, https://doi.org/10.1021/i160052a007.

[106] J.R. Scott, Theory and application of the parallel-plate plastimeter, Trans. Inst. Rubber Ind. 7 (1931) 169–186.

[107] A.P. Jackson, X.L. Liu, R. Paton, Squeeze flow characterisation of thermoplastic polymer, Compos Struct. 75 (2006) 179–184, https://doi.org/10.1016/j.compstruct.2006.04.064.

[108] T.G. Rogers, Squeezing flow of fibre-reinforced viscous fluids, J. Eng. Math. 23 (1989) 81–89, https://doi.org/10.1007/BF00058434.

[109] H.-R. Lin, S.G. Advani, Processing models and characterization of thermoplastic composite wound parts, Polym. Compos 18 (1997) 405–411, https://doi.org/10.1002/pc.10291.

[110] E.L. Wang, T.G. Gutowski, Laps and gaps in thermoplastic composites processing, Compos Manuf. 2 (1991) 69–78, https://doi.org/10.1016/0956-7143(91)90182-G.

[111] G.B. McGuinness, C.M. Ó Brádaigh, Characterisation of thermoplastic composite melts in rhombus-shear: the picture-frame experiment, Compos Part A Appl. Sci. Manuf. 29 (1998) 115–132, https://doi.org/10.1016/S1359-835X(97)00061-4.

[112] J.A. Barnes, F.N. Cogswell, Transverse flow processes in continuous fibre-reinforced thermoplastic composites, Composites 20 (1989) 38–42, https://doi.org/10.1016/0010-4361(89)90680-0.

[113] G.-P. Picher-Martel, A. Levy, P. Hubert, Compression molding of Carbon/Polyether ether ketone composites: squeeze flow behavior of unidirectional and randomly oriented strands, Polym. Compos 38 (2017) 1828–1837, https://doi.org/10.1002/pc.23753.

[114] V. Mhetar, L.A. Archer, Slip in entangled polymer melts. 1. General Features, Macromolecules 31 (1998) 8607–8616, https://doi.org/10.1021/ma980130g.

[115] V. Mhetar, L.A. Archer, Slip in entangled polymer melts. 2, Eff. Surf. Treat. Macromol. 31 (1998) 8617–8622, https://doi.org/10.1021/ma980130g.

[116] J. Engmann, C. Servais, A.S. Burbidge, Squeeze flow theory and applications to rheometry: a review, J. Non Newton Fluid Mech. 132 (2005) 1–27, https://doi.org/10.1016/j.jnnfm.2005.08.007.

[117] S.G. Hatzikiriakos, Progress in Polymer Science Wall slip of molten polymers, Prog. Polym. Sci. 37 (2012) 624–643, https://doi.org/10.1016/j.progpolymsci.2011.09.004.

[118] B. Barari, P. Simacek, S. Yarlagadda, R.M. Crane, S.G. Advani, Prediction of process-induced void formation in anisotropic Fiber-reinforced autoclave composite parts, Int J. Mater. Form. 13 (2020) 143–158, https://doi.org/10.1007/s12289-019-01477-4.

[119] P. Šimáček, S.G. Advani, A continuum approach for consolidation modeling in composites processing, Compos Sci. Technol. (2020) 186, https://doi.org/10.1016/j.compscitech.2019.107892.

[120] N.N. Kermani, V. Gargitter, P. Simacek, S.G. Advani, Gap filling mechanisms during the thin ply Automated Tape Placement process, Compos Part A 147 (2021), 106454, https://doi.org/10.1016/j.compositesa.2021.106454.

[121] J. Chen, K. Fu, Y. Li, Understanding processing parameter effects for carbon fibre reinforced thermoplastic composites manufactured by laser-assisted automated fibre placement (AFP, Compos Part A Appl. Sci. Manuf. 140 (2021), 106160, https://doi.org/10.1016/j.compositesa.2020.106160.

[122] J. Tierney, J.W. Gillespie, Modeling of heat transfer and void dynamics for the thermoplastic composite tow-placement process, J. Compos Mater. 37 (2003) 1745–1768, https://doi.org/10.1177/0021998303035188.
[123] T.K. Slange, W.J.B. Grouve, L.L. Warnet, S. Wijskamp, R. Akkerman, Towards the combination of automated lay-up and stamp forming for consolidation of tailored composite components, Compos Part A Appl. Sci. Manuf. 119 (2019) 165–175, https://doi.org/10.1016/j.compositesa.2019.01.016.
[124] M.A. Lamontia, M.B. Gruber, J. Tierney, J.W. Gillespie, B. Jensen, R. Cano, In Situ Thermoplastic ATP Needs Flat Tapes and Tows with Few Voids, 30th Int. SAMPE Eur. Conf., Paris, France, 2009, pp. 1–8.
[125] T. Centea, L.K. Grunenfelder, S.R. Nutt, A review of out-of-autoclave prepregs – material properties, process phenomena, and manufacturing considerations, Compos - Part A Appl. Sci. Manuf. 70 (2014) 132–154, https://doi.org/10.1016/j.compositesa.2014.09.029.
[126] B. Thorfinnson, T.F. Biermann, Production of void free composite parts without debulking, 31st Int. SAMPE Symp. (1986) 480–490.
[127] F. Sacchetti, W.J.B. Grouve, L.L. Warnet, I.F. Villegas, Effect of resin-rich bond line thickness and fibre migration on the toughness of unidirectional Carbon/PEEK joints, Compos Part A Appl. Sci. Manuf. 109 (2018) 197–206, https://doi.org/10.1016/j.compositesa.2018.02.035.
[128] J. Colton, J. Muzzy, S. Birger, H. Yang, L. Norpoth, Processing parameters for consolidating PEEK/carbon fiber (APC-2) composites, Polym. Compos 13 (1992) 421–426, https://doi.org/10.1002/pc.750130604.
[129] E. Courvoisier, Y. Bicaba, X. Colin, Water absorption in PEEK and PEI matrices. Contribution to the understanding of water-polar group interactions. AIP Conf Proc 1736 (2016) 1–5, https://doi.org/10.1063/1.4949611.
[130] C.M. Ma, S. Yur, -W. Environmental effects on the water absorption and mechanical properties of carbon fiber reinforced PPS and PEEK composites. Part II, Polym. Eng. Sci. 31 (1991) 34–39, https://doi.org/10.1002/pen.760310107.
[131] Q. Wang, G.S. Springer, Moisture absorption and fracture toughness of PEEK polymer and graphite fiber reinforced PEEK, J. Compos Mater. 23 (1989) 434–447, https://doi.org/10.1177/002199838902300501.
[132] D. Zhang, D. Heider, J.W. Gillespie, Volatile removal during out of autoclave processing of high performance thermoplastic composites. CAMX 2014 - Compos. Adv. Mater. Expo Comb. Strength, Unsurpassed Innov., Orlando, Floride, 2014.
[133] T.K. Slange, L. Warnet, W.J.B. Grouve, R. Akkerman, Influence of preconsolidation on consolidation quality after stamp forming of C/PEEK composites. ESAFORM, Americal Institute of Physics; 201, Nantes, FRANCE, 2016, https://doi.org/10.1063/1.4963578.
[134] T.K. Slange, Rapid Manufacturing of Tailored Thermoplastic Composites by Automated Lay-up and Stamp Forming A Study on the Consolidation Mechanisms, University of Twente, Enschede, The Netherlands, 2019. PhD Thesis.
[135] C.M. Stokes-griffin, P. Compston, T.I. Matuszyk, M.J. Cardew-hall, Thermal modelling of the laser-assisted thermoplastic tape placement process, J. Thermoplast. Compos Mater. (2013) 1–18, https://doi.org/10.1177/0892705713513285.
[136] C. Bas, A.C. Grillet, F. Thimon, N.D. Albérola, Crystallization kinetics of poly(aryl ether ether ketone): Time-temperature-transformation and continuous-cooling-transformation diagrams, Eur. Polym. J. 31 (1995) 911–921, https://doi.org/10.1016/0014-3057(95)00060-7.
[137] T.J. Chapman, J.W. Gillespie, R.B. Pipes, J.A.E. Manson, J.C. Seferis, Prediction of process-induced residual stresses in thermoplastic composites, J. Compos Mater. 24 (1990) 616–643, https://doi.org/10.1177/002199839002400603.
[138] J. Tierney, J.W. Gillespie, Modeling of in situ strength development tow placement process, J. Compos Mater. (2006) 40, https://doi.org/10.1177/0021998306060162.
[139] L. Ye, K. Friedrich, J. Kästel, Y.-W. Mai, Consolidation of unidirectional CF/PEEK composites from commingled yarn prepreg, Compos Sci. Technol. 54 (1995) 349–358, https://doi.org/10.1016/0266-3538(95)00061-5.
[140] J. Patou, R. Bonnaire, E.De Luycker, G. Bernhart, Influence of consolidation process on voids and mechanical properties of powdered and commingled carbon / PPS laminates, Compos Part A 117 (2019) 260–275, https://doi.org/10.1016/j.compositesa.2018.11.012.
[141] A. Levy, P. Hubert, Vacuum-bagged composite laminate forming processes: predicting thickness deviation in complex shapes, Compos Part A Appl. Sci. Manuf. 126 (2019), 105568, https://doi.org/10.1016/j.compositesa.2019.105568.
[142] P.P. Parlevliet, H.E.N. Bersee, A. Beukers, Residual stresses in thermoplastic composites—a study of the literature—part I: formation of residual stresses, Compos. Part A Appl. Sci. Manufact. 37 (2006) 1847–1857, https://doi.org/10.1016/j.compositesa.2005.12.025.
[143] Fink B.K., Gillespie J.W., Ersoy N.B. Thermal Degradation Effects on Consolidation and Bonding in the Thermoplastic Fiber-Placement Process. Army Res Lab 2000.
[144] T. Bayerl, M. Brzeski, M. Martı, R. Schledjewski, P. Mitschang, Thermal degradation analysis of short-time heated polymers, J. Thermoplast. Compos Mater. 28 (2015) 390–414, https://doi.org/10.1177/0892705713486122.
[145] F. Heinecke, C. Willberg, Manufacturing-induced imperfections in composite parts manufactured via automated fiber placement, J. Compos Sci. (2019) 1–24, https://doi.org/10.3390/jcs3020056.
[146] V. Dhinakaran, K.V. Surendar, M.S.H. Riyaz, M. Ravichandran, Review on study of thermosetting and thermoplastic materials in the automated fiber placement process, Mater. Today Proc. 27 (2020) 812–815, https://doi.org/10.1016/j.matpr.2019.12.355.
[147] H. Suemasu, Y. Aoki, S. Sugimoto, T. Nakamura, Effect of gap on strengths of automated fiber placement manufactured laminates, Compos Struct. 263 (2021), 113677, https://doi.org/10.1016/j.compstruct.2021.113677.
[148] D. Del Rossi, V. Cadran, P. Thakur, M. Palardy-sim, M. Lapalme, L. Lessard, Experimental investigation of the effect of half gap / half overlap defects on the strength of composite structures fabricated using automated fibre placement (AFP), Compos Part A 150 (2021), 106610, https://doi.org/10.1016/j.compositesa.2021.106610.
[149] S. Qian, X. Liu, Y. Ye, Q. Xu, T. Zhang, X. Li, Effect of gap and overlap fiber placement defects on the delamination behavior of L-shaped composite laminates, Compos Struct. 268 (2021), 113963, https://doi.org/10.1016/j.compstruct.2021.113963.
[150] G. Clancy, D. Peeters, V. Oliveri, R. O'Higgins, D. Jones, P.M. Weaver, Steering of carbon fiber/thermoplastic pre-preg tapes using laser-assisted tape placement, AIAA/ASCE/AHS/ASC Struct Struct Dyn Mater Conf 2018 (2018) 1–17. https://doi.org/10.2514/6.2018-0478.
[151] A. Rajasekaran, F. Shadmehri, Steering of carbon fiber/PEEK tapes using Hot Gas Torch-assisted automated fiber placement, J. Thermoplast. Compos Mater. 0 (2022) 1–29, https://doi.org/10.1177/08927057211067962.
[152] G. Struzziero, M. Barbezat, A. Antonios, Consolidation of continuous fibre reinforced composites in additive processes: a review, Addit. Manuf. 48 (2021), 102458, https://doi.org/10.1016/j.addma.2021.102458.
[153] A. Leon, C. Argerich, A. Barasinski, E. Soccard, F. Chinesta, Effects of material and process parameters on in-situ consolidation, Int J. Mater. Form. (2018), https://doi.org/10.1007/s12289-018-1430-7.